Analytica Chimica Acta

Review

Multifunctional nanoparticles: Analytical prospects

Alejandro Simón de Dios, Marta Elena Díaz-García*

University of Oviedo, Department of Physical and Analytical Chemistry, Faculty of Chemistry, Av. Julián Clavería, 8, 33006 Oviedo, Spain

ARTICLE INFO

ABSTRACT

Multifunctional nanoparticles are among the most exciting nanomaterials with promising applications in analytical chemistry. These applications include (bio)sensing, (bio)assays, catalysis and separations. Although most of these applications are based on the magnetic, optical and electrochemical properties of multifunctional nanoparticles, other aspects such as the synergistic effect of the functional groups and the amplification effect associated with the nanoscale dimension have also been observed. Considering not only the nature of the raw material but also the shape, there is a huge variety of nanoparticles. In this review only magnetic, quantum dots, gold nanoparticles, carbon and inorganic nanotubes as well as silica, titania and gadolinium oxide nanoparticles are addressed. This review presents a narrative summary on the use of multifuncional nanoparticles for analytical applications, along with a discussion on some critical challenges existing in the field and possible solutions that have been or are being developed to overcome these challenges.

© 2010 Elsevier B.V. All rights reserved.

Contents

1. Introduction

Over the past few decades, nanoscale particles have elicited much interest due to their distinct chemical, physical and biological properties. A variety of nanoparticles (NPs) with various shapes such as spheres, nanotubes, nanohorns and nanocages, made of different materials, from organic dendrimers, liposomes, gold, carbon, semiconductors, silicon to iron oxide, have already been fabricated and explored in many scientific fields, including chemistry, material sciences, physics, medicine and electronics [1–3]. At the nanoscale, the physical, chemical, and biological properties of materials differ fundamentally and often, unexpectedly, from their corresponding bulk counter part because of the quantum size effect, e.g. gold and silver nanoparticles are characterized by their ability to strongly absorb the visible light at definite wavelengths which depend on the size and the shape of the nanoparticles [4] whereas

* Corresponding author.
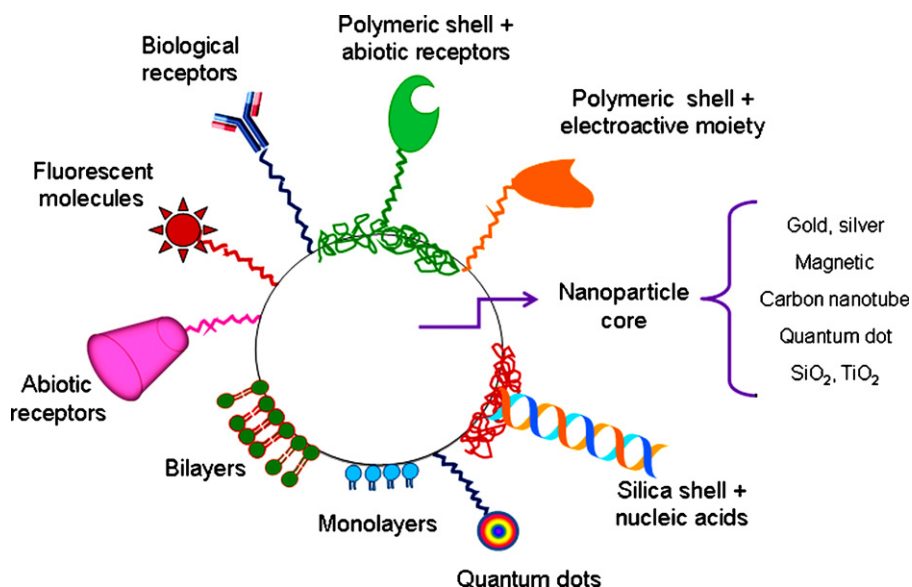E-mail address: medg@uniovi.es (M.E. Díaz-García).

Fig. 1. Multifunctional nanoparticle: all in one. The nanoparticle core can be also doped with a different nanoparticle and/or a dye.

the absorption of visible light in a large range from quantum dots induces the emission of visible light whose wavelength increases with the size of the nanoparticles [5].

The functionalization of nanoparticle surface is one method for tuning the overall properties of particles to fit targeted applications. The surface modification of nanoparticles by functional molecules/particles/polymers has different tasks to fulfil:

(a) stabilize the nanoparticles in solution to control the growth of the embryonic particles and determine their shape during the growth process
(b) provide functional groups at the surface for further derivatization
(c) enhancement of the nanoparticle solubilisation in various solvents to extend their application capabilities
(d) capping layers can modify the electronic, optical, spectroscopic and chemical properties of the particles, providing a plethora of controllable nanotools
(e) modify the capability to assemble the particles in specific arrays or the ability to target desired chemical, physical, or biological environments.
(f) improve the mechanical and chemical performance of the nanoparticle surface, e.g. protection against oxidation
(g) in some instances a reduction of their toxicity is achieved (e.g. cadmium based quantum dots)

Whereas mono functional nanoparticles provide a single function – a quantum dot can exhibit high fluorescence but it cannot be removed from a matrix using a magnetic field – multifunctional nanoparticles (MFNPs) are able to achieve a mixed effect using one system. In these systems variable strategies are use to attain a combination of targeting specificity, optimized optical-, electrical and/or magnetic properties and analysis capability. These general considerations are summarized in Fig. 1.

MFNPs are not a new nanotechnological innovation. Perusal of the literature demonstrates that the unique properties of MFNPs along with the "size effect" of nanoparticles, have already opened exciting avenues for developing new and advanced nanoparticle probes for biomedical imaging and drug delivery, which have great potential for therapy in areas, such as cancer, diagnostics and neuropathologies. Great effort is also devoted to characterization, understanding, and improvement of the structural properties of

such MFNPs nanostructures [6–9]. However, the unique features of these MFNPs remain practically unexplored in analytical chemistry and applications to the development of new analytical methodologies and/or devices with the aim of determining species in solution are really scarce.

The number of different type of nanoparticles is increasing rapidly; however, from the analytical standpoint they most can be classified into two major types. Particles that contain inorganic elements, usually metals and metal oxides, as a core (Fe_3O_4, semiconductors, gold, silver, TiO_2, SiO_2) and those that are based on organic molecules (carbon nanotubes, dendrimers, liposomes) as a major building materials. The aim of this paper is to direct attention to MFNPs, emphasizing the advances made in this field in the last five years and to outline the potential applications in analytical chemistry. Structural functionalities and applications of magnetic, quantum dots, gold, silica, titania and gadolinium oxide nanoparticles as well as carbon and inorganic nanotubes will be addressed.

2. Multifunctional magnetic nanoparticles

Superparamagnetic nanoparticles represent one of the most exciting prospects in current analytical nanotechnology because they can be easily separated from a matrix by using a magnetic field without retaining residual magnetism (no agglomeration) after removal of the field. Several types of iron oxides have been used in the field of magnetic NPs; mostly includes Fe_3O_4 (magnetite), α-Fe_2O_3 (hematite, weakly ferromagnetic or antiferromagnetic), γ-Fe_2O_3 (maghemite, ferrimagnetic), FeO (wüstite, antiferromagnetic), ε-Fe_2O_3 and β-Fe_2O_3, among which magnetite and maghemite are popular candidates since its biocompatibility have already proven in bio labelling and bio separation [10].

Iron oxide nanoparticles or magnetic nanobeads are a kind of nanomaterial which might play an important role in the construction of electrochemical biosensors [11]. Firstly, iron oxide nanoparticles have a very large surface area and good biocompatibility. Furthermore, these magnetic particles are especially designed for concentration, separation, purification, and identification of molecules and specific cells and are particularly suitable for integration in micro fluidic devices [12–14].

Uncoated magnetic nanoparticles in themselves have some limitations: (a) they have a large surface to volume ratio and therefore possess high surface energies; as a result, they tend to aggregate
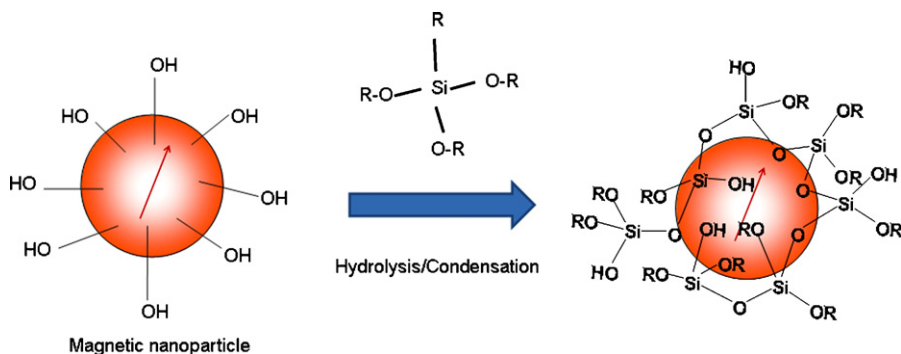
Fig. 2. Silane surface coating of a magnetic nanoparticle.

so as to minimize the surface energies, (b) iron oxide nanoparticles have high chemical activity and get easily oxidized when exposed to air that results in loss of magnetic properties and dispersibility, (c) undergo biodegradation (with subsequent changes in magnetic properties). To address such issues, the development of a proper surface coating to protect and keep the stability of magnetic iron oxide NPs is required. The strategies comprise grafting of or coating with organic molecules, including small organic molecules or surfactants, polymers, and bio molecules, or coating with an inorganic layer, such as silica, metal or non-metal elementary substance, metal oxide or metal sulphide [15]. Practically, it is worthy that in many cases the protecting shells not only stabilize the magnetic iron oxide NPs, but can also be used for further functionalization and to promote the performance of the nanoparticles as recognition elements in sensing and (bio)chemical assays. Due to the amount of literature available, mainly in the medical field, we will focus on selected analytical examples to illustrate novel concepts and promising applications of multifunctional magnetic NPs.

Silica is often employed as coating material over the surface of NPs as silica is chemically inert, promotes the dispersion of the NPs, have a high surface silanol concentration which facilitates a wide variety of surface reactions and the binding of bio molecules (antigen-antibodies, peptides, proteins, nucleic acids, enzymes), metals and polymers [16]. The physicochemical mechanism of the silane agent modifying on the surface of iron oxide NPs according to Arkles [17] is depicted in Fig. 2.

The hydroxyl groups on the iron oxide NPs surface reacted with the alkoxy groups of the silane molecules leading to the formation of Si–O bonds and leaving the terminal functional groups available for further immobilization of other molecules. In general, the behaviour of silica coated magnetic nanoparticles is related to the thickness of their respective silica shells. Normally, a thicker silica shell reduces the inter-particle interaction and super paramagnetism is preserved although it is also accompanied by a sacrifice in saturation magnetization (M_s). The reduction in M_s value could be attributed to the lower density of the magnetic component in the silanized nanoparticle sample [18]. For instance, a 15 nm silica coating caused saturation magnetization to decrease from 81.2 emu g^{-1} for bare Fe$_3$O$_4$ nanoparticles to 49.7 emu g^{-1} [19]. The 3-aminopropyltriethoxysilane (APTEOS), p-aminophenyltrimethoxysilane (APTS) and mercaptopropyltriethoxysilane (MPTES) agents are mostly employed for providing the amino and sulphydryl groups, respectively.

While using alkoxysilanes is a very useful approach to start NPs functionalization, a drawback accompanied by its reaction route is the presence of some remaining silanol groups in the product owing to the incompletion of the dehydration reaction. These silanol groups are highly reactive [20,21] and, unless they are end-capped with a suitable reagent, their presence might cause further condensation reactions during the period of storage and usage of

the formed nanocomposites [20]. Consequently, some alternative methods have been developed to prepare multifunctional nanoparticles and examples will be considered in more detail below.

2.1. Magnetic nanoparticles functionalized with molecularly imprinted polymers

Molecular imprinting is a well-established method for the synthesis of polymeric materials with specific recognition properties for template molecules [22,23]. The approach involves polymerization of functional monomers and a cross-linker around a print molecule. Once the template was extracted, receptor sites are present in the material with functional and shape complementary to the template. Today's concept of molecular imprinting has been widely recognized as the most promising methodology for the preparation of different tailor-made materials with selective binding. Due to their high selectivity, mechanical strength, resistance against acids, bases, organic solvents, and high pressures and temperatures, as well as the low cost and ease for preparation, molecularly imprinted polymers (MIPs) were developed for extensive applications such as solid phase extraction (SPE), chromatography, enzymatic catalysis, and sensor technology [22–24].

Generally, MIPs have been prepared via bulk polymerization in the form of monolithic blocks. Grinding the blocks into a particulate product of controlled size is necessary in most analytical applications. To avoid that tedious and time consuming process, an increasing number of polymer formats and methods of polymerization have been developed, such as imprinting of beads, suspension polymerization, production of thin films or membranes, phase inversion, surface imprinting (for imprinting large molecules), electrosynthesized and nanosized imprinted polymers. In spite of all these potential functionalities and properties, only a few studies on MIP materials in conjugation with magnetic nanoparticles have been published up to now.

Ansell and Mosbach [25] first reported the use of molecularly imprinted polymer-magnetic iron oxide composite materials for (S)-propranolol competitive radioligand binding assays using a magnet to separate polymer from solution. Magnetic beads were directly added to the pre-polymerization mixture. Although magnetic beads were not nanosized, the concept was demonstrated and authors concluded that recognition properties of the imprinted polymer particles were not affected by inclusion of iron oxide.

More recently, Zhang and co-workers [26] have reported the synthesis of a magnetic molecularly imprinted polymer (M-MIP) of bisphenol A (BPA) by miniemulsion polymerization. The morphological and magnetic characteristics of the M-MIP were characterized by FTIR (Fourier Transform Infrared Spectroscopy), TEM (Transmission Electron Microscopy) and vibrating sample magnetometry. The magnetic Fe$_3$O$_4$ nanoparticles were modified with methacryloxypropyltrimethoxysilane (MAPS) in

order to provide surface polymerizable functional groups. The template, the functional monomer (2-vinylpyridine, 2-VP), the cross-linking monomer (ethyleneglycoldimethacrylate, EGDMA) and Fe$_3$O$_4$@MAPS were mixed. After ultrasonication, addition of a sodium dodecylsulphate solution and degassing, the initiator (azo-bis-isobutyronitrile, AIBN) was added. The resulting polymeric microspheres were washed and the template molecules removed by Soxhlet extraction. These multifunctional nanoparticles were used in a molecularly imprinted solid-phase extraction approach assisted by magnetic separation to extract BPA from environmental water and milk samples. High-performance liquid chromatography with UV detection was employed to determine BPA after the extraction. For water samples, the developed method exhibited a limit of detection (LOD) of $14\,\mathrm{ng\,L^{-1}}$, a relative standard deviation of 2.7% (intraday), and spiked recoveries ranging from 89% to 106%. For milk samples, the LOD was $0.16\,\mathrm{\mu g\,L^{-1}}$, recoveries ranged from 95% to 101%, and BPA was found in four samples at levels of $0.45–0.94\,\mathrm{\mu g\,L^{-1}}$. Authors concluded that the method not only provided a rapid and reliable analysis but it also overcame problems with conventional solid-phase extraction (SPE), such as the packing of the SPE column and the time-consuming nature of the process of loading large-volume samples.

Chen and co-workers [27] have developed magnetic nanoparticles coated with a molecularly imprinted film against estrone. Synthesized Fe$_3$O$_4$ nanoparticles were firstly coated with a shell of silica using tetraethoxysilane (TEOS), after which the silica modified magnetic nanoparticles were reacted with a silane derivative of estrone, (CH$_3$CH$_2$-O)$_3$-Si-(CH$_2$)$_3$-NH-COO-estrone, to create a second shell of molecularly imprinted sol–gel. Estrone was extracted by hydrolysis. The use of magnetic nanoparticles allowed the easy removal of reagents, the washing of materials and the separation of final product by simply applying a magnetic field. The multifunctional nanoparticles were characterized by physical and chemical methods. Although no applications were described in the paper, authors recommended the potentialities of these hybrid nanoparticles for biochemical separations, cell sorting, recognition elements in biosensors and drug delivery.

The synthesis of magnetic molecularly imprinted polymer nanoparticles for aspirin recognition and drug controlled release have been performed by Wang and Zhu et al. [28]. In their approach, magnetic nanoparticles were chemically modified with a double bond by the direct reaction between γ-methacryloxypropyltrimetroxysilane (γ-MPS) and hydroxyl groups at the Fe$_3$O$_4$ nanoparticle surface. The double bond guided the formation of methacrylic acid-based molecularly imprinted polymer at the nanoparticle surface by radical polymerization. The resulting product was collected by an external magnetic field and aspirin was removed using a methanol/acetic acid mixture. The applicability of the material was demonstrated by *in vitro* controlled release of aspirin: in the first two hours, about 50% of the total aspirin loaded was released from magnetic MIPs, while 85% of adsorbed aspirin was released from the non-imprinted magnetic nanoparticles. No analytical applications of these multifunctional nanoparticles were addressed.

Yang and co-workers [29] have described the synthesis of molecularly imprinted magnetic nanowires within the pores of nanoporous alumina membrane. Theophiline, the template molecule, was immobilized on the pore walls of a nanoporous alumina membrane. The nanopores were then filled with a prepolymerization mixture containing the superparamagnetic MnFe$_2$O$_4$ nanocrystallites. After polymerization, the alumina membrane was removed by chemical dissolution, leaving behind magnetic polymer nanowires that contain theophylline binding sites uniquely residing at the surface. The resulting magnetic imprinted polymer nanowires (saturated magnetization of $1.97\,\mathrm{emu\,g^{-1}}$) were capable of binding theophylline more strongly than the non-imprinted nanowires.

2.2. Magnetic nanoparticles functionalized with host–guest systems

Molecular recognition by host–guest systems has been successfully developed and recognition of neutral organic molecules by synthetic receptors is a topic of current interest not only in supramolecular- but also in analytical chemistry. Macrocyclic hosts such as crown ethers, cryptands, cyclophanes, calixarenes and cucurbiturils have been synthesized and received much attention, opening a wide range of opportunities for new supramolecular chemistry and materials. Among them, cyclodextrins (CDs) are the most important and promising macrocyclic hosts because they are water-soluble natural products, inexpensive, commercially available, non-toxic and readily functionalized [30–32]. Cyclodextrins (CD), composed of six (α), seven (β), or eight (γ) D-glucopyranose units, possess truncated cone-shaped hydrophobic cavities, which are capable of binding various organic, inorganic, and biological molecules to form stable host–guest inclusion complexes in aqueous solution. Each CD has its own ability to form host–guest inclusion complexes with specific guest molecules, an ability which depends on a proper fit of the guest molecule into the hydrophobic CD cavity. The principal advantages of natural CDs as recognition moieties are: (1) a well-defined chemical structure, yielding many potential sites for chemical modification; (2) the availability of CDs of different cavity sizes; (3) low toxicity and (4) the protection of the included molecule from biodegradation and quenching (when dealing with luminescent molecules). These properties are also expected to be useful in the assembly of magnetic nanosystems.

As a proof of the concept, recently, a protocol for the preparation of a novel versatile nanocomposite possessing superparamagnetism has been described by Wu et al. [33]. The synthesis of the functionalized nanoparticles followed the scheme: (a) Fe$_3$O$_4$ magnetic nanoparticles were functionalized with oleic acid (OA) via a two-step method [32], (b) monotosyl-polyethyleneglycol (monotosyl-PEG) silane was then immobilized on the OA-coated magnetic nanoparticles, (c) in order to introduce β-CD onto the magnetic nanoparticles, the tosyl termini of polyethyleneglycol (PEG) molecules were displaced by ethylenediamine-containing β-CD through a nucleophilic substitution reaction. The multifunctional nanoparticles were then physically and chemically characterized. Authors applied the system to the detection of dopamine in water solution by dispersing the multifunctional nanoparticles in the aqueous solution containing dopamine to form the inclusion complex. Then, the magnetic nanoparticles, using an external magnet, were absorbed onto ITO (indium tin oxide) for the electrochemical detection of dopamine. Results demonstrated that due to both the electrocatalytic effect of the magnetic nanoparticles and the host–guest effect of β-CD, dopamine could be detected with high sensitivity.

2.3. Magnetic nanoparticles functionalized with avidins

In addition to macrocycles, affinity biological systems are used to functionalize magnetic NPs. For instance, the avidin/biotin system. The egg-white glycoprotein avidin and its non-glycosylated bacterial analogue streptavidin are two evolutionarily unrelated proteins that bind the vitamin biotin with remarkably high affinity constants ($K_d = 10^{-15}\,\mathrm{M^{-1}}$). The bond formation between biotin and avidin/streptavidin is very rapid and, once formed, is unaffected by pH, organic solvents and other denaturing agents. Both, avidin and streptavidin, have essentially irreversible biotin-binding properties since bound biotin can only be released by denaturing the subunits of the proteins. These unique features are the

basis of avidin/streptavidin-biotin technology, which has evolved into a universal tool in various fields of the biological and analytical sciences [34–37]. Some notable differences exist between these two proteins. Avidin is a glycoprotein and contains one disulphide bridge and two methionine residues, whereas streptavidin is non-glycosylated and devoid of any sulphur containing residues. Whereas avidin bears a single tyrosine residue, the content of tyrosine residues in streptavidin is relatively high (six per subunit).

Among the various magnetic NP composites developed to date, streptavidin-immobilized magnetic particles have shown great analytical potential due to the stability of the biotin-streptavidin interaction and the resulting ability to separate target molecules specifically and efficiently. Recently, Hafaid et al. [38] have explored the development of impedimetric immunosensors based on magnetic iron nanoparticles functionalized with streptavidin to which a biot-tag anti-D-dimer reduced antibody (Fab fragment Biot-ScAc) was bound using a biotin-streptavidin interaction. SPR (Surface Plasmon Resonance) analysis showed a deviation on the measured angle during antigen-antibody recognition whereas label free detection using by EIS (Electrochemical Impedance Spectroscopy) allowed monitoring variation of polarization resistance. Compared to immobilization of antibody on bare gold surface using aminodecanethiol SAM (Self Assembled Monolayers), antibody immobilization on magnetic nanoparticles permitted to reach lower detection limits for the antigen: $500 \, pg \, mL^{-1}$ instead of $1 \, ng \, mL^{-1}$ to in the case of EIS (Electrochemical Impedance Spectroscopy) and $300 \, ng \, mL^{-1}$ instead of $4.5 \, \mu g \, mL^{-1}$ in the case of SPR. Thus, the approach permitted to improve the sensitivity: from $257.3 \, \Omega \, cm^2 \, \mu g^{-1} \, mL$ to $1871 \, \Omega \, cm^2 \, \mu g^{-1} \, mL$ in the case of EIS and from $0.003 \, \mu g^{-1} \, mL$ to $0.094 \, \mu g^{-1} \, mL$ in the case of SPR. According to the authors the use of the iron oxide nanoparticles amplified the response signal, due to an increase in the thickness of the layer of antibody from 0.4 to 1.2 nm, from where, an increase of the grafting density of antibody on the surface resulted in larger amounts of antigen linked to the specific sites [38].

Erdem, Piskin et al. [39] have investigated the applicability of streptavidin carrying magnetic nanoparticles in electrochemical nucleic acid sensor systems. Magnetite (Fe_3O_4) nanoparticles were coated with a carboxylic acid containing polymer layer and streptavidin molecules were immobilized onto the surfaces of the nanoparticles via these functional groups. For electrochemical detection of sequence specific DNA hybridization and its selectivity studies, a biotinylated hepatitis B Virus (HBV) wild type probe was immobilized onto the nanoparticles. An electrochemical nucleic acid sensor system composed of a disposable graphite sensor, pencil graphite electrode (PGE) and differential pulse voltammetry (DPV) was used for measurement of guanine oxidation signals in solutions containing no target, the complementary target, a single-base mismatch target, and non-complementary target oligonucleotides. A significant guanine oxidation signal was observed with the complementary target due to complete hybridization, while with single-base mismatch target, the signal at the same conditions was negligible. In the case of the non-complementary target, there was also a low mean signal (due to non-specific interactions). The detection limit (S/N = 3) was found as $43.11 \, pmol \, mL^{-1}$ target concentration obtained in 20 min hybridization time.

The synthesis of oleic acid stabilized monodisperse iron oxide nanoparticles coated with biotinylated poly(N-isopropylacrylamide) (b-PNIPAAm) has recently been described by Narain et al. [40]. The ability of the biotin terminal groups on the b-PNIPAAm-coated nanoparticles to interact with streptavidin was confirmed by fluorescence and surface plasmon resonance. Although no analytical application was described, it was found that the b-PNIPAAm-coated iron oxide nanoparticles bound with high affinity to streptavidin in solution or when the streptavidin was immobilized on a surface. Also, it was demonstrated that the binding of the biotin ligands on the surface of the temperature-responsive magnetic nanoparticles to streptavidin could be turned on and off as a function of temperature.

2.4. Magnetic nanoparticles functionalized with biological receptors

Surface enzyme immobilization has become an important topic in nanodevices [41–46], especially for electrochemical biosensing where the main challenge is to combine the features required for self-sufficient operation in the same electrode. The manipulation of nanostructured materials in conjunction with biological molecules has led to the development of a new class of hybrid modified electrodes in which both enhancement of charge transport and biological activity preservation may be obtained [47].

A novel glucose biosensor was recently prepared by Li et al. [48] with Fe_3O_4 nanoparticles containing Prussian blue (PB) and glucose oxidase (GOx) attracted to the surface of solid paraffin carbon paste electrode by magnetic force. The glucose oxidase was covalently conjugated to the amine-modified nanoparticles. Because of the high reactivity of hydrogen peroxide with the Prussian blue contained in the glucose biosensor, the hydrogen peroxide formed during the enzymatic reaction with glucose was measured by the current generated to determine the glucose concentration. The biosensor showed high sensitivity, selectivity, stability and short response time. It exhibited a linear response to glucose over the range from 5.0×10^{-7} to 8.0×10^{-5} M with a detection limit of 1.0×10^{-7} M. Reductive substances in biological samples did not interfere with the detection of glucose, so that the biosensor was also used to determine the glucose concentration in human blood samples.

Similarly, a phenol biosensor was developed by Yu and co-workers [49] based on the immobilization of tyrosinase on the silica surface of modified magnetic $MgFe_2O_4$ nanoparticles, which were further modified with amino groups on their surface. The resulting magnetic bio-nanoparticles were attached to the surface of a carbon paste electrode (CPE) with the help of a permanent magnet. The immobilization matrix provided an adequate microenvironment for retaining the tyrosinase activity. Phenol was determined by direct reduction of bio catalytically generated quinone species at $-150 \, mV$ versus SCE. The resulting phenol biosensor could reach 95% of steady-state current within 20 s and exhibited a high sensitivity of $54.2 \, \mu A \, mM^{-1}$, as a result of the high tyrosinase loading in the immobilization matrix. The linear range for phenol determination was from 1×10^{-6} to 2.5×10^{-4} M and a detection limit of 6.0×10^{-7} M was obtained. The stability and the application of the biosensor to phenol determination in industrial waste water were evaluated with excellent results.

Irudayaraj and co-workers [50] successfully bound cholesterol oxidase (CHO) to magnetic nanoparticles (Fe_3O_4) via carbodiimide activation. FTIR spectroscopy was used to confirm the binding of CHO to the particles. The binding efficiency was between 98 and 100% irrespective of the amount of particles used. Kinetic studies of the free and bound CHO revealed that the stability and activity of the enzyme were significantly improved upon binding to the nanoparticles. Furthermore, the bound enzyme exhibited a better tolerance to pH, temperature and substrate concentration. The activation energy of CHO activity was reduced upon binding onto Fe_3O_4 nanoparticles. No analytical application is described, however, the work concluded that the stability and activity of CHO could be enhanced via attachment to magnetic nanoparticles and, consequently, it may contribute to better uses of the enzyme in various biological and clinical applications.

Going one step beyond, it was also found that the magnetic properties of the iron-oxide core could be further exploited

Table 1
Analytical applications of magnetic multi-function nanoparticles.

Nano-particle	Core shell	Analytical application	Comments	Refs.
$CoFe_2O_4$	Prussian blue nanoparticle-doped silica	Aflatoxin B1 in food: Red paprika specimens assayed	Simple, rapid, highly sensitive, specific, and no sample pre-concentration	[53]
Fe_3O_4	Silica + PS + MIP Template: Bovine hemoglobin	Separation of proteins	Imprinted superparamagnetic nanoparticles easily reach the adsorption equilibrium	[54]
Fe_3O_4	Fungal mycelium + chitosan imprinted shell. Template: Cu(II) ions	Separation of copper ions	Nanocomposite efficient, low-cost, convenient for separation, reusable.	[55]
Fe_3O_4	Mercapto silica	SPE of Cd, Cu, Hg, and Pb traces, biological and environmental samples	LODs for Cd, Cu, Hg and Pb: 24, 92, 107, and 56 $pg\,L^{-1}$, respectively	[56]
Fe_3O_4	Amino silica + β-cyclodextrin	Promising applications in bioseparations	Superparamagnetic nanocomposite with high saturation magnetization	[57]
Fe_3O_4	Streptavidin	No analytical applications	Two types of biotinylated analytes: agarose beads and BSA	[58]
Fe_3O_4	Avidin	Separation of oligonucleotides and DNA	Stable suspensions of avidin-coated magnetic nanoclusters	[59]
Fe_3O_4	Silica+carboxylic groups	Separation of proteins	Cytochrome C (12,000 Da), Rnase B (15,000 Da), Myoglobin (17,000 Da)	[60]
Fe_3O_4	Covalent binding of hepatitis B surface antibody	Immunovoltametric determination of hepatitis B surface antigen	LOD 0.06 $ng\,mL^{-1}$, higher than that of ELISA assay	[61]
Fe_3O_4	Gold nanoparticles	Staphylococcal enterotoxin B in food	Magnetic nanogold microspheres as immunosensing probe	[62]
Fe_3O_4	Silica + surfactants	Pre-concentration of phenols, water samples	Concentration factors of 1600 over 800 mL of different environmental water samples	[63]
Fe_3O_4	HMS	Extraction of DDT from aqueous media	Fe_3O_4@HMS materials: high adsorption capacity and fast adsorption rate	[19]

MIP: molecularly imprinted polymer; PS: polystyrene; SPE: solid phase extractions; LOD: limit of detection; BSA: bovine serum albumin; ELISA: enzyme linked immunosorbent assay; DDT: dichloro-diphenyl-trichloro-ethane; HMS: hexagonal mesoporous silica.

for the development of high sensitive immunoassay-based dip-sticks. These devices make use of bio-functionalized magnetic nanogold microspheres as detection reagent in combination with gold nanoparticles. Knopp and co-workers [51] have developed a novel membrane-based lateral-flow immune-dip-stick assay for the fast screening of aflatoxin B_2 (AFB_2) as a model compound in food samples. The detector reagent consisted of magnetic nano-Fe_2O_3 particles as core and gold nanoparticles bio-functionalized with monoclonal anti-AFB_2 antibodies as recognition layer. A major advantage of the approach was that the visual detection limit (cut-off value) of the magnetic-gold modified-based dip-stick immunoassay with 0.9 $ng\,mL^{-1}$ AFB_2 was about threefold lower compared to a conventional immune-dip-stick test using gold nanoparticles as detection reagent. Without expensive equipment, qualitative results (yes/no) could be obtained within 15 min. The assay was evaluated with AFB_2 spiked or naturally contaminated samples ($n = 8$), including peanuts, hazelnuts, pistachio and almonds, with excellent results when compared with those obtained by high performance liquid chromatography (HPLC). Authors highlighted that the assay did not give false negative results. By controlling the target antibody the proposed format may be easily extended for use with other food relevant toxins and thus represents a versatile detection method.

2.5. Magnetic nanoparticles functionalized with nucleic acids

A simple and effective procedure for the surface modification of pure magnetite and silica-coated magnetite with an–NH_2 linker using aminopropyltriethoxysilane (APTS) as the surface modification agent has been reported by Bruce et al. [52]. The amine activated surface was used to covalently link specific oligonucleotide (or single strand DNA) onto the magnetic particles and thereby generate "bioactive" nanoparticles. Surface amine groups were converted to aldehyde groups via treatment with glutaraldehyde. These groups were reacted with amine-modified oligonucleotides, in this case a 50-amine modified dC6dT25 oligonucleotide, that was used for the specific capture of fluores-

cent labelled complementary single stranded DNA in solution. The efficiency for capture of complementary sequences was directly related to the surface density of amine groups. Authors highlighted that optimization of the silanization surface activating reaction and systematic studies on the effect of reaction variables in the production of high performance materials were still necessary.

Some other examples of magnetic nanoparticles-molecular recognition systems are summarized in Table 1.

2.6. Magnetic nanoparticles functionalized with fluorescent probes

Superparamagnetic nanoparticles have a high potential as supporting media for functional molecules (e.g. fluorescent dyes) for use in different science applications (e.g. assays, magnetic resonance imaging, magnetic cell separation, magnetic oligonucleotide and nucleic acid separation). Besides the magnetic separation and targeting of nanoparticles, different methods for their detection become more and more important. For example, a multifunctional fluorescent superparamagnetic nanoparticle separable with a conventional permanent magnet and tagged with a biomolecule allows for magnetic separation and magnetic targeting in life science applications in combination with the sensitive method of fluorescence detection.

Gun'ko and co-workers have recently presented an overview of bimodal "two-in-one" magnetic-fluorescent nanocomposite materials which combine both magnetic and fluorescent properties in one entity, in particular those with potential applications in biotechnology and nanomedicine [64]. Based on the structure and synthesis strategies, the authors classified fluorescent/magnetic nanocomposites in eight types: (i) a magnetic core coated with a silica shell containing fluorescent components; (ii) polymer-coated magnetic nanoparticles functionalized with a fluorescent moiety; (iii) ionic aggregates consisting of a magnetic core and fluorescent ionic compounds; (iv) fluorescently labelled bilipid-coated magnetic nanoparticles; (v) a magnetic core covalently bound to a fluorescent entity via a spacer; (vi) a magnetic core directly
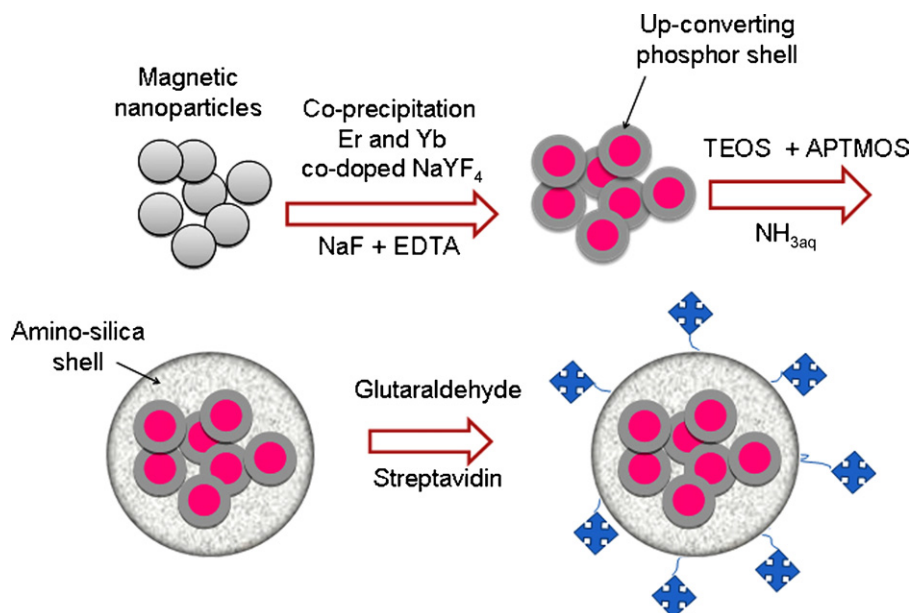
Fig. 3. Steps for the synthesis of streptavidin immobilized up-conversion phosphor magnetic nanoparticles. TEOS: tetraethoxy-orthosilane; APTEOS: amino-propyl-triethoxysilane; EDTA: ethylenediaminetetraacetic acid. Adapted from Ref. [66].

coated with a semiconducting shell; (vii) magnetically doped QDs and (viii) nanocomposites, which consist from magnetic nanoparticles and QDs encapsulated within a polymer or silica matrix. Authors concluded that, despite of all recent progress made, the fluorescent-magnetic nanocomposite area is still in its infant stage and significant efforts are needed for further development of these materials and their utilization.

The idea of combining the magnetic response with fluorescence has been reported in only a few articles with analytical purposes (e.g. separations and labelling). He et al. [65] synthesized hydrophilic high-luminescent magnetic nanocomposites composed of both fluorescent clusters (quantum dots, QDs) and magnetic nanoparticles. In order to explore potential applications authors selected biotin–streptavidin as molecular recognition system and competitive inhibition experiments in which luminescent/magnetic nanoparticles labelled with streptavidin were mixed with free streptavidin and biotin-horseradish peroxidase. Results demonstrated a good competitive inhibition relationship for streptavidin concentrations between 23 and 92 nM, thus confirming that streptavidin on the surface of the luminescent magnetic nanoparticles was bioactive. The role of the QDs in these nanocomposites was not explained.

Chen, Guo et al. [66] have described a method of preparing up-converting fluorescent magnetic nanoparticles with covalently coupled streptavidin. As illustrated in Fig. 3, sodium yttrium fluoride, co-doped with ytterbium and erbium, was co-precipitated on iron oxide nanoparticles in the presence of a chelator, EDTA. The magnetic nanoparticles were so coated with an up-converting phosphor shell. The magnetic/fluorescent nanoparticles were then coated with an amino-silane layer and, after activation with glutaraldehyde, the particles were covalently coupled with streptavidin. Protein arrays were used to confirm the successful binding of streptavidin. Authors demonstrated the success of streptavidin immobilization on the hybrid nano-particle by its specific binding with an array of biotinylated IgG spots on a glass slide. A home-built CCD biochip scanner with an external 980 nm laser and an infrared filter were used to detect the infrared-to-visible up-conversion fluorescence on the glass slide. Signal from positive control spots assured the working state of the glass slide and scanner, whereas the absence of any signal from negative control spots demonstrated

that non-specific absorption was low. Up-conversion fluorescence signal from the biotinylated IgG spots came from streptavidin-coated hybrid nanoparticles bound to the glass slide through the specific biotin/streptavidin interaction. Authors conclude that (a) these streptavidin-coated up-conversion fluorescent magnetic nanoparticles can be readily coupled with bio-molecules such as antibodies, proteins and nucleic acids, etc., via streptavidin/biotin interaction and (b) they are potentially useful in a variety of areas because they can be simultaneously manipulated with an external magnetic field and characterized in situ using fluorescence microscopy or confocal scanning microscopy.

Yuan and co-workers [67] have recently described the synthesis and application of multifunctional nanoparticles possessing magnetic, long-lived fluorescence and bio-affinity properties. The multifunctional nanoparticles have been prepared by copolymerization of a conjugate of an alkoxysilane bound to a fluorescent Eu^{3+} complex, free APTEOS and TEOS in the presence of poly(vinylpyrrolidone) (PVP) stabilized magnetic Fe_3O_4 nanoparticles (<10 nm). The presence of amino groups on the nanoparticle's surface allowed the nanoparticles to be labelled with transferrin and their use for staining cultured HeLa cells (immortal cell line derived from human epithelial cervical carcinoma). Results showed that non-specific adsorption of the nanoparticles was negligible: after free fluorescent nanoparticles were incubated with HeLa cells, fluorescence microscopy and time resolved fluorescence microscopy demonstrated that no nanoparticles were inside the cells. On the contrary, the labelled transferrin fluorescent nanoparticles incubated with HeLa cells were transported into them via the transferrin–transferrin receptor interaction on the cell surface and the receptor-mediated endocytosis. Analytical characteristics of the method revealed the usefulness of time-resolved fluorescence imaging technique to eliminate the interference of cellular autofluorescence and sample background fluorescence.

Micron-sized, monodisperse, superparamagnetic, luminescent composite poly(glycidyl methacrylate) (PGMA) microspheres with functional amino-groups were successfully synthesized by Chang et al. [68]. The process of preparation included different steps: (a) preparation of monodisperse poly(glycidyl methacrylate) microspheres by dispersion polymerization method, (b) modification of poly(glycidyl methacrylate) microspheres with ethylene diamine
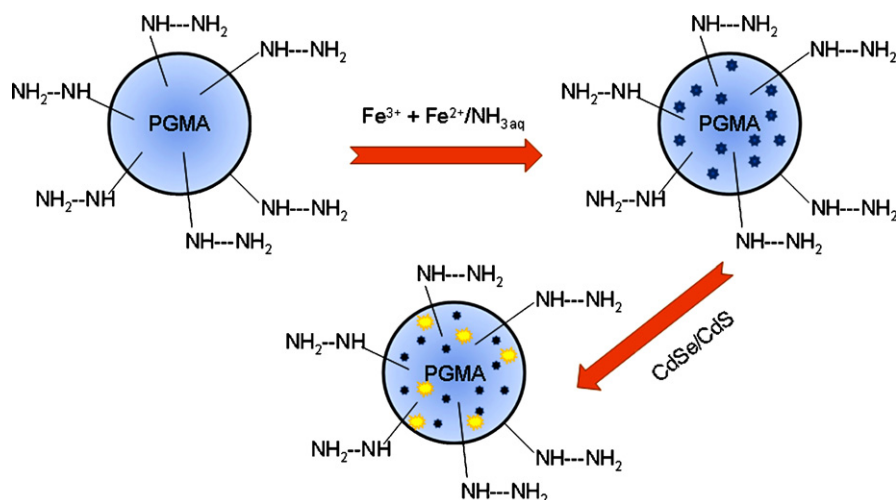
Fig. 4. PGMA nanoparticles functionalized with magnetic and luminescent nanoparticles PGMA = poly(glycidyl methacrylate. Adapted from Ref. [68].

to form amino-groups, (c) inclusion of iron ions (Fe^{2+} and Fe^{3+}) inside the microspheres and subsequently precipitation with ammonium hydroxide to form magnetite (Fe_3O_4) nanoparticles within the polymer microspheres and (d) infiltration of CdSe/CdS core-shell QDs into magnetic polymer microspheres (Fig. 4). These fluorescent magnetic nanoparticles are type viii, according to Gun'ko and co-workers [64]. The composite microspheres were bright enough, easily observed using a conventional fluorescence microscope and were easily separated from solution by magnetic decantation using a permanent magnet. Although authors claimed that these new multifunctional composite microspheres were promising in a variety of bio analytical assays involving luminescence detection and magnetic separation, no analytical applications were reported.

Tang and co-workers [69] have developed a similar approach based on magnetic and fluorescent (CdTe QDs) multifunctional chitosan nanoparticles to design an innovative cefradine delivery system. The composite nanoparticles showed favourable superparamagnetic and fluorescent properties and stimulus responsive controlled drug release. On the other hand, authors indicated that it was easy to functionalize the nanoparticles with targeting components such as tumour specific ligands and monoclonal antibodies which can further enhance their targeting potential.

In 2007, Chen et al. [70] reported for the first time the spectral characteristics of Rhodamine B/silica/modified magnetic nanoparticles. These multifunctional nanoparticles were found to be highly fluorescent although no analytical applications were addressed. Later, a simple and reproducible method was developed by Chang et al. [71] to synthesize a novel class of Fe_3O_4/SiO$_2$/Rhodamine B/SiO$_2$ composite nanoparticles. These multifunctional nanoparticles were found to be highly luminescent, photostable and superparamagnetic. The colour of the luminescence was successfully tuned by incorporating different dyes into the nanoparticles, which may have potential use for multiplex bioanalysis and imaging. Authors did not apply the system to real sample analysis; however, they highlighted the potential of these nanoparticles as promising candidates for use in bioassays, not only for the possibility to use different fluorescent dyes but also because the outer shell of silica could be tuned by changing the concentration of the silicon precursor during the synthesis.

Although no fluorescent, Liu et al. [72] fabricated Fe_3O_4/poly(N-isopropylacrylamide)/chitosan multiresponsive composite beads (400 nm) via emulsion polymerization in two steps. Firstly, Fe_3O_4 nanoparticles were modified with oleic acid and then they were embedded in chitosan and N-isopropylacrylamide. The nanopar-

ticles showed magnetic, thermo- and pH-sensitive properties. No analytical applications were performed; however, authors concluded that these composite nanospheres, with multiresponsive properties, show great promise in biomedical applications.

In conclusion, the synergy of combined magnetic nanoparticles for analyte separation and recognition/detection techniques has several analytical advantages over other labels. The magnetic properties of the nanoparticles are stable over time, in particular, because the magnetism is not affected by reagent chemistry, no significant magnetic background is usually present in common samples and magnetic fields are not screened by aqueous reagents or (bio)materials. In addition, magnetism may be used to remotely manipulate the magnetic particles.

3. Multifunctional gold nanoparticles

Gold nanoparticles are particularly attractive in analytical applications because they have unique optical properties (i.e. exhibit a strong absorption band in the UV–visible region and resonance light scattering). The physical origin of this light absorption by gold nanoparticles is the coherent oscillation of the conduction electrons induced by the interacting electromagnetic field [73]. As nanoparticles have a high surface area to volume ratio, the plasmon frequency is highly sensitive to the dielectric (refractive index) nature of its interface with the local medium, leading to colorimetric changes of the dispersions [73–75].

The simplest and by far the most commonly used preparation for gold nanoparticles (AuNPs) is the aqueous reduction of HAuCl$_4$ by sodium citrate at boiling point [76]. This method produces monodisperse spherical AuNPs in the 10–20 nm diameter range. Although sodium citrate is the most common reducing agent, metal nanoparticles can also be synthesized by the use of borohydride and other reducing agents [77,78]. Particles synthesized by citrate reduction are nearly monodisperse spheres of a size controlled by the initial reagent concentrations. They have a negative surface charge as a consequence of a weakly bound citrate coating and are easily characterized by their plasmon absorbance band (at about 520 nm for 15 nm particles). Nanoparticles from other noble metals may also be prepared by citrate reduction, such as silver particles from AgNO$_3$, palladium from H$_2$ [PdCl$_4$], and platinum from H$_2$ [PtCl$_6$] [79–81]. The similarities in the preparation of these different metal colloids allow the synthesis of mixed-metal particles, which may have functionality different from each individual metal. For example, the reduction of suitable mixtures of noble metal salts can lead to alloy or mixed grain particles [82].

Most of the techniques reported for immobilization of (bio)molecules onto AuNPs surface are based on Au-S covalent bond formation between the (bio)molecules and the gold atoms on the particle surface. This approach makes use of sulphur containing ligands, e.g. thiol, disulphide and thiolester. Goodman and Rotello [83] have reviewed monolayer-protected gold nanoparticles in the multivalent binding of biomolecular targets and their role as a design element for particle-target recognition, in the development of advanced model systems and in catalysis. Although the affinity between the gold and silica is weaker than those between magnetic nanoparticles or quantum dots and silica, covering of AuNPs with silica as starting point for further functionalization is also possible. To afford this, an anchor precursor such as γ-trimethoxysilyilpropylmethacrylate (MPTS) or APTEOS is required for the surface targeted growth of silica on gold nanoparticles [84,85] and then, the hydrolysis of TEOS (or other alkoxysilane precursor) through either the sol–gel technology or the reverse micro emulsion method is performed to form a second silica layer. Although the silica shell may prevent the aggregation of AuNPs, so far, the application of the gold–silica hybrid in analytical approaches is limited. In the following, we provide an overview of recent examples of multifunctional AuNPs-based assays. Recently, Chang et al. [86] have reviewed the use of DNA functionalized of gold nanoparticles in bioanalysis while Chen et al. [87] reviewed the current use of AuNPs in nanomedicine and nanosensing. Multifunctional gold nanoparticles were not considered.

Gold nanoparticles can be rendered luminescent by luminol which emits light when oxidized ((electro)chemiluminescence). Tillement et al. [88] demonstrated that dihydrolipoic acid (DHLA), a dithiol obtained by the reduction of thioctic acid, appeared very attractive for the stabilization and the further functionalization of gold nanoparticles (Fig. 5).

The ionisable carboxylic acid groups ensured, for pH ≥ 8, the water solubility of DHLA-capped gold (Au@DHLA) nanoparticles and the stability of the resulting colloid by electrostatic repulsions. Luminol was successfully grafted to 5 nm sized gold nanoparticles coated by dihydrolipoic acid through the formation of amide linkage between the amino group of luminol and the carboxylic acid moiety of the diethylenetriaminepentaacetate (DTPA) ligand. This study showed that gold nanoparticles exerted a catalytic activity on the luminol oxidation and therefore on the light emission from luminol. In fact, it was found that luminol-functionalized particle was nine times as bright as a single luminol molecule [88]. The use of these luminescent particles as biological probes with a lower threshold of detection was envisaged.
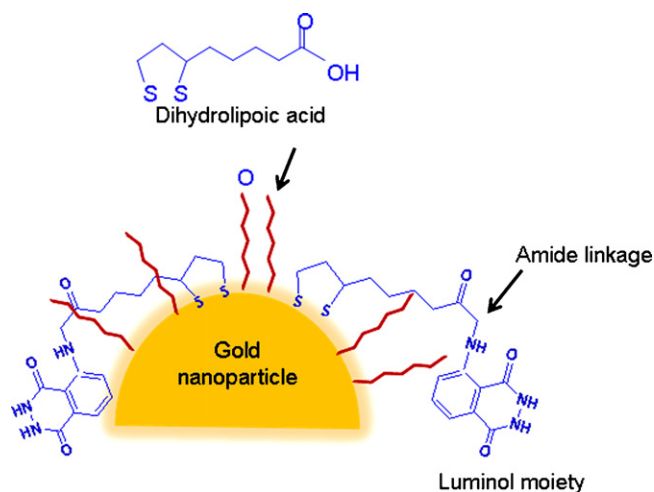

Fig. 5. Gold nanoparticles functionalized with DHLA/DHLA-luminol amide. DHLA = dihydrolipoic acid.

Gold nanoparticles can be rendered also phosphorescent. Thomas et al. [89] have modified the surface of AuNPs by capping the surface with monothiol derivatives of 2,2′-dipyridyl (AuNP-D). The high local concentration of the chelating ligands (ca. 5 M) around the AuNPs makes these particles "ion sponges". The complex formed with Eu(III)/Tb(III) ions rendered the nanoparticles phosphorescent. The red-emitting AuNP-D-Eu(III) and the green-emitting AuNPs-D-Tb(III) complexes exhibit long lifetimes of 0.36 ms and 0.7 ms, respectively. These phosphorescent multifunctional nanomaterials were further used as sensors for metal cations. It was observed that upon addition of alkaline earth and transition metal ions a drastic decrease in phosphorescence took place due to the isomorphous substitution of the lanthanide ions.

Zhang and co-workers [90] have recently developed a sensitive electrochemical DNA sensor based on nanoporous gold (NPAu) electrode and multifunctional encoded AuNP. The NPAu electrode was prepared with a simple strategy by which silver was dissolved from a commercially available 9-carat white gold leaf (Ag/Au alloy, 50:50 wt%) in nitric acid. During etching, silver atoms were selectively dissolved and the gold atoms left behind assembled into the 3D porous structure. The DNA biosensor was fabricated by immobilizing capture probe DNA on the NPG electrode and hybridization with target DNA, which further hybridized with the reporter DNA (multifunctional encoded AuNP coupled with [Ru(NH$_3$)$_6$]$^{3+}$). The
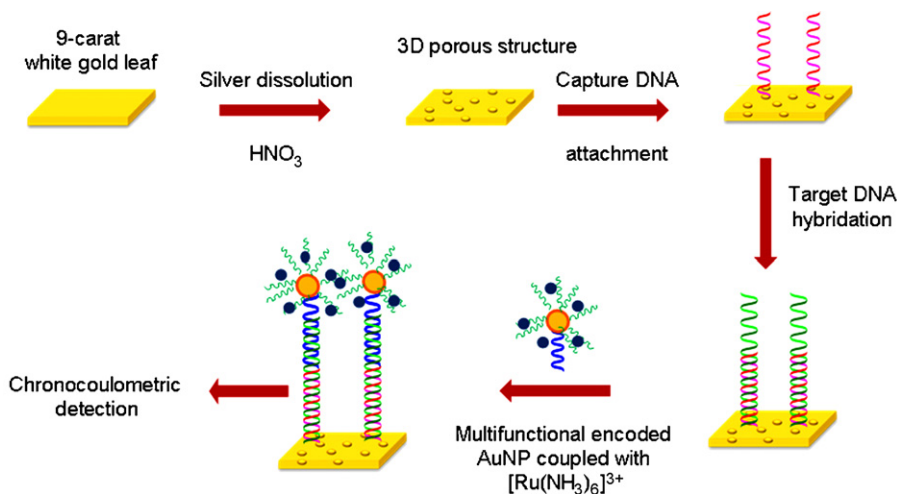

Fig. 6. DNA Biosensor based on nanoporous gold electrode and multifunctional encoded DNA–Au bio bar codes. Adapted from Ref. [90].
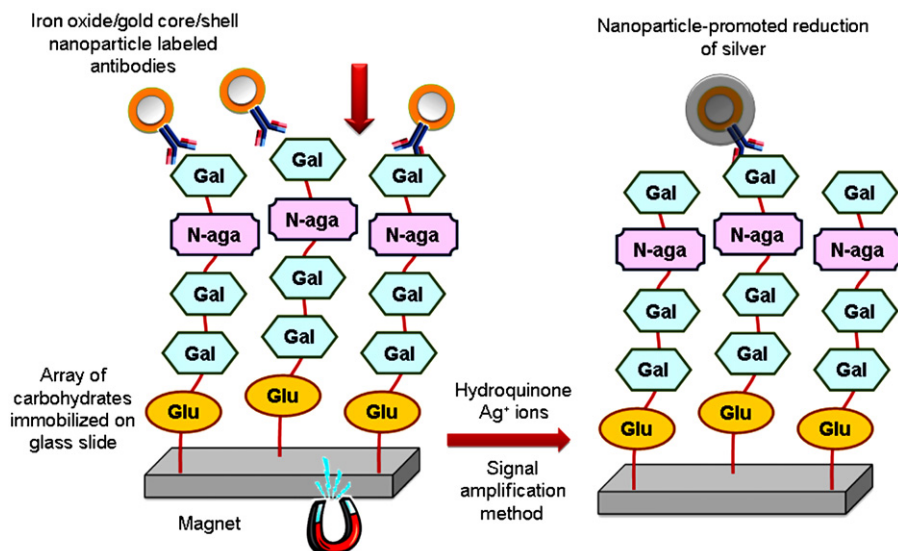
Fig. 7. Scheme of iron oxide/gold core/shell nanoparticle-based assays: binding of core/shell nanoparticle labelled antibodies with tumour associated carbohydrate antigens is facilitated by application of a magnetic field, followed by a silver enhancement step. The final reading was performed with a conventional flatbed scanner. Adapted from Ref. [92].

AuNP contained two kinds of bio bar-code DNA, one was complementary to the target DNA, while the other was not, reducing the cross-reaction between the targets and reporter DNA on the same AuNP. Electrochemical signals of $[Ru (NH_3)_6]^{3+}$ bound to the reporter DNA via electrostatic interactions were measured by chronocoulometry (Fig. 6).

Taking advantage of dual-amplification effects of the AuNPs electrode and multifunctional encoded AuNP, this DNA biosensor could detect the DNA target quantitatively, in the range of 8.0×10^{-17}–1.6×10^{-12} M, with a limit of detection as low as 28 aM, and exhibited excellent selectivity even for single-mismatched DNA detection. The NPG-based biosensor could be regenerated by incubation of the modified electrode in hot water (90 °C) for 1 min, by which hybridized DNA was removed via thermal denaturation. After the regeneration procedure was performed three times, the AuNPs-based biosensor almost retained its original hybridization efficiency. Authors highlighted the advantages of this biosensor: (a) the fabrication of NPAu electrode was quite simple and economical, avoiding the use of template, (b) cross-reaction was avoided by the use of AuNPs containing two DNA bio bar codes and (c) the approach could be extended to its application in ultramicroassay techniques.

Li et al. [91] reported the synthesis of bifunctional Au-Fe$_3$O$_4$ nanoparticles. Due to the chemical linkage of Au nanoparticles, the resulting bifunctional Au-Fe$_3$O$_4$ nanoparticles were easily modified with other functional molecules to realize various nanobiotechnological separations and detections. In their work, authors demonstrated that Au-Fe$_3$O$_4$ nanoparticles could be modified with nitrilotriacetic acid through Au–S interaction and used to separate proteins simply with the help of a magnet. Bradford protein assay and sodium dodecylsulphate–polyacrylamide gel electrophoresis were performed to examine the validity of the separation procedure. The separated proteins maintained catalytic as confirmed by the phosphate determination method. Authors highlighted the efficiency of such a material in protein separations and suggested that its use could be extended to magnetic separation of other bio substances. According to the authors, this synthetic strategy paves the way for facile preparation of diverse bifunctional and even multifunctional nanomaterials.

Inspired by the concept of the bio barcode assay, Wong, Wu et al. [92] introduced iron oxide/gold core/shell nanoparticles as a means to increase complexity and functionality in a scanometric array detection system. Core/shell nanoparticles consist of discrete domains of different materials and, thus, can exhibit the properties of different components in the same structure. With this idea, the authors developed an ultrasensitive glycans array using iron oxide/gold core/shell nanoparticles conjugated with antibodies or proteins (see Fig. 7).

A magnetic field was applied to bring nanoparticle labelled proteins or antibodies from a solution to an array of carbohydrates immobilized on glass slides and to drive them to encounter the carbohydrates at very low concentration. In this approach, iron oxide/gold core/shell nanoparticles combine, in a single entity, the ability of magnetic property for enrichment, surface modification, and signal enhancement by depositing silver on the gold surface of core/shell nanoparticles. Well-defined recognition systems, namely, mannose derivatives (Man1, Man4, and Man9) with a mannose binding lectin (Concanavalin A) and a stage-specific embryonic antigens-3 (SSEA-3) with a monoclonal antibody (anti-SSEA-3) were chosen to establish this detection tool. Array systems were conducted to determine surface dissociation constant and binding specificity for qualitative and quantitative analysis of carbohydrate-protein and carbohydrate antibody interactions. When coupled with a signal amplification method based on nanoparticle-promoted reduction of silver, the sensitivity of an iron oxide/gold core/shell nanoparticle-based assay reached to subattomole level in carbohydrate detection. Authors conclude that the core-shell nanoparticle assay was a promising analytical method in carbohydrate analysis with the advantages of decreased sampling volume, improved test sensitivity, and reduced cost as compared to fluorescence-based assays. In clinical applications, this ultrasensitive assay for detecting low levels of cancer-associated carbohydrate antigens can be a powerful diagnostic tool for early diagnosis of diseases.

Au nanoparticles modified by SAMs with mixed carboxylic acid and amine functional groups were developed by Shyue et al. [93]. Based on electrostatic interactions, molecules could be triggered to adsorb/desorb by changing the environmental pH around the tunable isoelectric point (IEP) of the nanoparticles (between 3.2 and 7.3). These engineered nanoparticles were synthesized in a single-phase system based on the reduction of HAuCl$_4$ by NaBH$_4$ in ethanol with a mixture of 16-mercaptohexadecanoic acid and 8-amino-1-

octanethiol that formed the SAM on the synthesized nanoparticles. Although no analytical applications were described, potential use of these multifunctional AuNPs was envisaged for molecule transportation (where the pH range is limited) due to their ability to flip surface charge at a specific pH to trigger the adsorption or desorption of molecules.

Recently, Shi et al. [94] have developed a facile approach to fabricating multifunctional dendrimer-stabilized gold nanoparticles (Au DSNPs) for cancer cell targeting and imaging. In their work, amine-terminated dendrimers pre-functionalized with folic acid (FA) and fluorescein isothiocyanate (FI) were complexed with Au (III) ions, followed by acetylation of the amine groups on the dendrimer surfaces. This one-step process resulted in the spontaneous formation of 6 nm sized AuNPs stabilized by multifunctional dendrimers bearing both targeting and imaging functionalities. Results demonstrated that the FA- and FI-functionalized dendrimer AuNPs were able to specifically target to cancer cells expressing high-affinity FA receptors *in vitro*. Authors claimed that the approach may be extended to other targeting molecules, providing a unique nanoplatform for targeting and imaging of a variety of biological systems.

A particularly elegant study by Boal and Rotello [95] describes the evolution of an optimized flavin binding site on AuNPs surface containing two different thiols functionalized with pyrene and diaminopyridine moieties, respectively, diluted by a matrix monolayer of octanethiol. The binding of flavin to diaminopyridine by hydrogen bonding was enhanced by a close pyrene unit, which should provide an additional binding interaction by aromatic stacking. Pyrene and diaminopyridine moieties were randomly distributed over the AuNPs surface and hence not necessarily close enough to show a synergistic binding effect for flavin: However, over a 73 h time period a rearrangement of the binding sites (random surface diffusion of the pyrene and diaminopyridine units) took place, giving rise to a 71% increase in the binding constant. The slow rearrangement suggested that it is not simply the thiol chains moving in space to maximize interactions, but actual movement of the bound chains on the particle surface to maximize the free energy of the system. This was an important advance which may lead to the development of a new approach to artificial receptor design similar to molecular imprinting [84]. It also confirms that multifunctional AuNPs are dynamic systems that do not only readily undergo ligand place exchange reactions but are also capable of remarkable re-organisation processes in their ligand shell.

Layer by layer (LBL) assembly is a simple technique that allows the construction of thin films by sequential exposure of polycationic and polyanionic solutions in the nanoscale. This approach has been performed for the construction highly stable enzyme biosensors based on AuNPs. Schneider and Decher [96] used the LBL approach to develop highly stable multifunctional AuNPs with positive and negative polyelectrolytes just controlling the electrostatic interactions. AuNPs were coated with a layer of positively charged redox polymer (as electrochemical functionality) and glucose oxidase (as bio functionality). The results shown in this work revealed good potential control in the electrophoretic deposition of the modified nanoparticles and the response of these modified multifunctional nanoparticles to glucose, studied on microelectrode configurations, showed a great enhancement of the signal recorded. These results demonstrate the potential of this modified AuNPs to be integrated in microelectrode arrays for the production of electrochemical sensing devices or multifunctional modified nanoreactors.

When gold nanoparticles aggregate, an enhanced resonance light scattering (RLS) is observed. This has been exploited by Diaz-Garcia et al. [97] to determine lysine in dietary supplements. The interaction of mercaptoundecanoic acid capped AuNPs with Eu^{3+} ions resulted in AuNPs surface plasmon spectral changes. At the

same time, the europium ions (complexed with acetate ions in buffer solution) fluorescence at 590 and 620 nm was quenched. Non-radiative energy transfer from excited Eu(III) to the nearby AuNPs through binding with the S (CH$_2$)$_{10}$COO- groups was proposed as non-radiative decay channel for the excited ions. On the other hand, it was observed that the light scattering of the AuNPs/Eu^{3+} system was enhanced upon addition of amino acids, particularly when lysine was added. Interplasmon coupling phenomena suggested that the functionalized nanoparticles were brought together upon addition of the lysine.

In a recent study, Pradeep et al. [98] have developed fluorescent three-dimensional (3D) super lattices of dansylglutathionate/N-acetylglutathionate protected gold nanoparticles, with potential applications in molecular detection. Morphologies of the superlattice crystals were examined using scanning electron microscopy (SEM) and most of the crystals observed were triangular in shape. Authors utilized the fluorescence of dansylglutathione gold superlattice crystals for the selective detection of bovine serum albumin (BSA) in the nmol L^{-1} range, based on the selective binding of the naphthalene ring of the dansyl moiety with BSA. According to the authors, these systems can be considered as a new class of functional materials for which it is possible to tune their functionality based on the requirements of a given application and can be used as an excellent platform on which to explore several interesting phenomena such as biomolecular detection, SERS, and gas sensing.

Gold nanoparticles conjugated with molecular beacons (MBs) have become interesting in DNA detection. Molecular beacons (MBs) have been widely used in nucleic acid diagnostic technology since their introduction in 1996 by Tyagi and Kramer [99]. MBs are single-stranded nucleic acid sequences composed of three different functional domains: (i) a target-recognition loop region of about 15–30 bases flanked by (ii) two short complementary stem sequences and (iii) a fluorophore/quencher pair.

The short complementary stems (4 to 7 base pairs) function as lockers to maintain the closed hairpin structure and bring the quencher nearby the fluorophore in a few nanometers' distance. The fluorophore and the quencher act as fluorescence resonance energy transfer based switches. When the donor fluorophore is in its excited state, the energy is transferred via a non-radiative long-range dipole-dipole coupling mechanism (energy transfer, FRET) to the acceptor quencher which is in close proximity (typically <10 nm) to it. Consequently, the fluorophore/quencher pair is normally in the "fluorescence off" state. In the presence of the target (complementary) DNA, the stem-loop unfolds and the fluorophore/quencher switchs to the "fluorescence on" state (see Fig. 8). The use of MBs as fluorescent signaling mechanism offers several advantages [100]: (i) the light-up signaling mechanism allows MBs to perform highly sensitive detection and monitoring of nucleic acids in real time. This detection-without-separation approach is particularly useful in those situations where it is either impossible or undesirable to extract the probe–target hybrids from an excess of the unbound probes; (ii) their relatively high signal-to-background ratio, providing higher sensitivity of detection compared to other conventional fluorescent probes. Upon hybridization to its target, a well-designed MB can generate as high as 200-fold fluorescence enhancement under optimal conditions; (iii) MBs are extraordinarily target-specific and are able to differentiate as low as single-mismatched base pair sequences. This selectivity is a direct result of their hairpin conformation, as the stem hybrid acts as an activation energy barrier to the loop-target hybrid.

In spite of these advantages, an important drawback of MBs is the low quenching efficiency of the molecular quencher. When the molecular quencher is replaced with Au NPs, the quenching is much more efficient, resulting in a more sensitive probe. So, Dubertret et al. [101] used a 3′-amino-5′-thiol-modified ssDNA oligomer to anchor the probe oligonucleotide to commercially available 1.4-nm
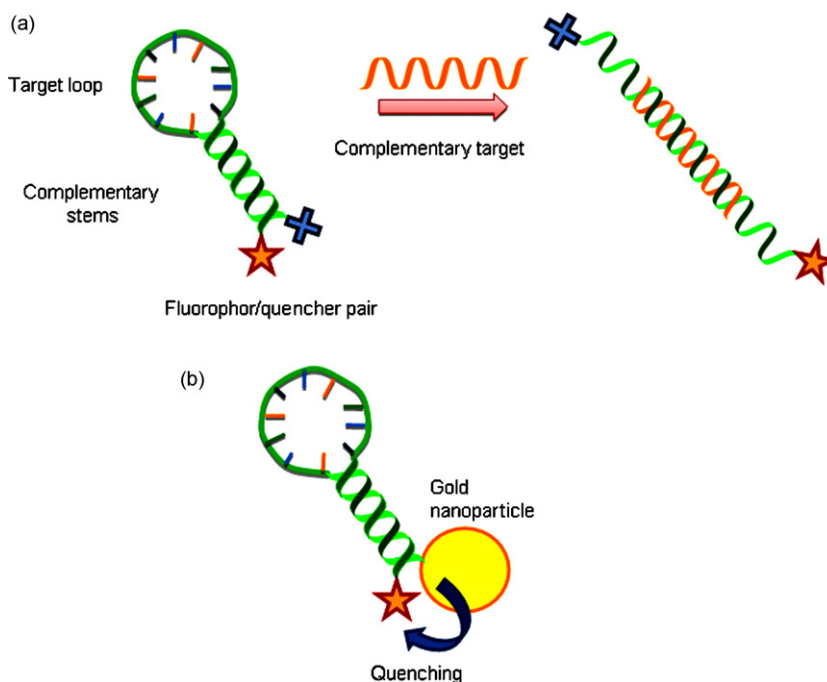
Fig. 8. (a) Molecular beacon signalling mechanism, (b) gold nanoparticle as efficient quencher of molecular beacon.

gold clusters containing a single maleimido group in their ligand shell and subsequent coupling with an amino-reactive fluorophore. This construct resulted in a quenched loop conformation that could be opened by hybridization, resulting in a fluorescence increase. The analytical performance of the hybrid molecular beacon was optimized by determining the quenching efficiency (QE) for several dyes. The QE was defined as the difference in fluorescence between the open duplex and the intramolecularly closed beacon. The best QE value (ca. 99.5%) was obtained for rhodamine 6G, indicating that the fluorescence signal of the beacon increased about 200-fold upon hybridization with the complementary target. The gold-oligomer-dye hybrids were applied to the detection of single mismatches in DNA and competitive hybridization assays revealed that the ability to detect single base mutations was about 8-fold greater than with conventional molecular beacons while the sensitivity of detection was enhanced up to 100-fold [101,102].

Gold NPs have been also used to create structures with MB function but without the stem-loop configuration. In this approach Nie et al. [103] used a 3′ thiol group to anchor the probe oligonucleotide to 2.5-nm AuNPs at one terminus and the strong physisorption of a 5′ fluorophore to anchor the other terminus. The AuNPs function as both a nano-scaffold and a nano-quencher (efficient energy acceptor). This hybrid bio/inorganic construct was found to spontaneously assemble into a constrained arch-like conformation on the particle surface and binding of target molecules resulted in a conformational change, which restored the fluorescence of the quenched fluorophore. Unlike conventional molecular beacons with a stem-and-loop structure, the nanoparticle probes did not require a stem. Authors claim that in comparison with the organic quencher Dabcyl (4,4′-dimethylaminophenyl azo benzoic acid), AuNPs offered unique structural and optical properties for new applications in biosensing and molecular engineering [103].

Sha et al. [104] have developed a molecular beacon format assay in which encoded nanowire particles were used to achieve multiplexing, demonstrating the principle with the detection of five viral pathogens: Hepatitis A virus, Hepatitis C virus, West Nile Virus, Human Immune Deficiency virus and Severe Acute Respiratory Syndrome virus. Oligonucleotides were designed com-plementary to a target sequence of interest containing a 3′ universal fluorescent dye (TAMRA, 5-(and-6)-carboxytetramethylrhodamine succinimidyl ester) and a 5′ thiol caused the oligonucleotides to self-assemble onto the metal nanowire. The single-stranded oligonucleotide contained a self-complementary hairpin stem sequence of 10 bases that forced the 3′ fluorophore to come into contact with the metallic nanowire surface, thereby quenching the fluorescence. By using differently encoded nanowires, each conjugated with a different oligonucleotide sequence, multiplexed DNA assays were possible using a single fluorophore, from a multiplexed reverse transcription-polymerase chain reaction (RT-PCR). Decoding of the nanowire striping pattern indicated which DNA sequence was present.

Aside from being a more efficient quencher, the gold NPs have also been used as scaffolds to carry multiple hairpins–something that is not possible with molecular quenchers. Song et al. [105] have demonstrated that large nanoparticles can accommodate tens of nucleotides on their surface, whereas small nanoparticles can only accommodate one or two. Authors were able to load approximately 44 nucleotides bearing different coloured fluorophores onto a single large gold nanoparticle. Each colour of fluorophore (FAM, Cy5 or Rox) targets a specific tumour-suppressor gene (p16, p21 or p53). The multicolour beacon produced the characteristic fluorescence when it bound to the designed targets: p16 produced the blue colour of FAM emission, p21 produced the red of Cy5 and p53 produced the orange of Rox. Moreover, the molecular beacons exhibited very fast response, achieving fluorescence recovery of up to 90% within 5 min.

While most of these multifunctional MB-AuNP assays are conceptually straightforward and elegant, a number of fundamental measurements are required to determine the optimum design for the assay. For example, the choice of fluorescence dye in any molecular beacon-based experiment can have a large impact on the attainable results [101,104]. The challenge is to find a dye that have ideal quenching properties, but without interfering with the analytical determination. Also, factors that influence molecular beacon surface coverage on metal nanoparticles and the impact of coverage on beacon performance in hybridization assays is another challenge
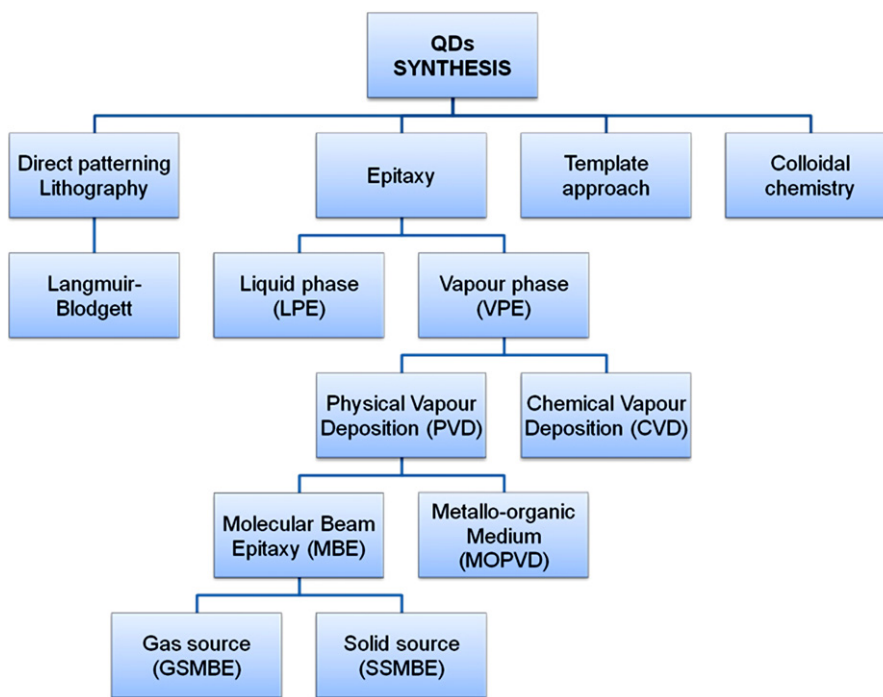
Fig. 9. Methods for QDs fabrication.

as surface attachment of MBs would enable not only a wide range of surface-based transduction strategies (optical, electrochemical), but also spatial arraying, substantially increasing the degree of multiplexing possible [106]. Finally, a drawback in the applicability of such multifunctional AuNPs in routine diagnostics are currently a consequence of the limited physicochemical stability of the metal clusters, their ligand shell, and the chemical linkage between the clusters and the DNA.

4. Multifunctional quantum dots

Quantum dots are colloidal fluorescent semiconductor nanocrystals, roughly spherical and typically have unique optical, electronic and photophysical properties that make them appealing in promising applications in biological labeling, imaging, and detection and as efficient fluorescence resonance energy transfer donors [107]. The most broadly applied quantum dots are composed of CdS and CdSe, i.e. of a combination of II–VI elements. Also other sulphides and selenides in addition to oxides, halides and tellurides have been reported [108,109]. In addition, combinations of III–V elements, (InP and InAs) have been utilized [110,111].

The size of a quantum dot is between 2 and 10 nm in diameter. Beyond this size, the quantum confinement effect is lost, and fluorescence is not observed. Compared to conventional small molecule luminophores, quantum dots are brighter and feature high quantum yields. Also, as quantum dots of different composition show emission spectra of distinct nuances [112], harnessing these characteristics could enable multiplexed assays as described by Soman and Giorgio [113]. Given that a quantum dot surface can be activated with a multitude of reactive moieties, a single crystal of 5 nm in diameter may act as a solid support for two to five molecules according to Chan and Nie [114]. All these characteristics make quantum dots excellent contrast agents for imaging and labels for bioassays. A number of reviews on the fabrication, properties, and applications of QDs have been reported recently [115–117].

Different synthetic routes can be employed for the preparation of QDs (see Fig. 9):

(a) Direct patterning; for example, CdSe QDs were prepared by using a modified hydrophobic–hydrophilic PDMS surface. The hydrophilic monomer was stamped on a hydrophobic PDMS to generate pattern of hydrophobic–hydrophilic PDMS surface [118].

(b) Lithography-based techniques, a combination of electron beam lithography and etching [119].

(c) Epitaxy-based methods, in which ordered growth of a crystalline material takes place on top of a pre-existing crystalline substrate, are affordable approaches for growing high quality crystalline in quantum devices applications [120,121]. There are many kinds of epitaxy, the main difference being the supply of source atoms: the source could be a molecular beam, gas, liquid or even an amorphous solid layer.

(d) Template approaches, in which many different materials such as porous alumina, polymer gel, surfactant, activated carbon and carbon fiber have been used as templates to synthesize different kinds of nanostructured porous materials [122].

(e) Colloidal chemistry, a straightforward ("one-pot") approach that may be conducted by rapid injection of semiconductor precursors into hot and vigorously stirred specific organic solvents containing molecules that can coordinate with the surface of the precipitated QD particles [123–125] or even by a hydrothermal approach in high-temperature water [126]. While colloidal chemistry is mostly used for the synthesis of QDs for (bio)analytical chemistry applications, QDs prepared by the remaining approaches are widely used in optoelectronics (lasers, infrared photodetectors) and nanotechnologies. Organically capped QDs produced by colloidal chemistry are of high quality; however, for a number of analytical applications, in particular clinical/biological related, QDs have to meet several criteria: (a) most of the biomolecules, e.g. enzymes, peptides, nucleic acids, exist in aqueous environments and most of the samples are also aqueous: modifying the surface of QDs to be hydrophilic and compatible to varieties of (bio)molecules and samples is a key issue; (b) labeling (bio)molecules and cells with QDs requires surface modification, making it water compati-

ble; (c) for *in vivo* applications, non-toxic performance of QDs is crucial.

Several strategies have been designed for rendering QDs water-soluble: functionalization with water soluble ligands, silanization, titania, organic dendrons, cysteines, dihydrolipoic acid, encapsulation with block-copolymer micelles, with amphiphilic polymers, amphiphilic polymers conjugated with poly(ethylene glycol) and surface coating with phytochelatin-related peptides. In addition, quantum dots can be conjugated to biological molecules such as proteins, oligonucleids, small molecules, etc., which are used to direct binding of the quantum dots to areas of interest for bio-labelling and biosensing. A review illustrating the methods for chemical surface modification of QDs has been recently published [127].

As in the case of magnetic nanoparticles, silica is widely used for coating QDs. A primary goal of silica coating is the possibility of isolating of QDs in order to reduce their toxicity as toxic heavy metal ions can be released from quantum dots, such as Cd^{2+} [128–130]. Silica nanoparticles, which themselves are well known to be non-toxic nanomaterials [131], are effective blocking materials for quantum dots as demonstrated by Kirchner et al. [132] in a cell proliferation assay in which no toxicity was observed from the silica coated quantum dots (concentration of 30 μM of surface Cd atoms), while the bare quantum dots killed almost all the cells.

The improvement in surface properties of quantum dots is also an advantage of a silica coating. In fact, silica surface improves the QDs hydrophylicity and provides a convenient scaffold for further surface modifications. The silica surfaces can be easily functionalized by silica precursors, such as MPTS and APTEOS, to provide amine or thiol reactive groups. The functionalized surfaces can be further decorated with antibodies and proteins based on well-established chemical methods [133].

Coating the QDs' surfaces with suitable ligands and/or receptors can have a strong effect on its luminescent response to specific chemical species. In fact, the presence of the analyte can quench or enhance the nanocrystal luminescence, depending on the functionalization strategy. Several approaches have been performed to use QDs as sensors for metal ions. In a recent paper by Ruedas-Rama et al. it was reported the development of multi-ion sensing using different combinations of QDs with selected ionophores or organic fluorophores embedded in a polymeric composite material [134]. In their approach, authors explored the differences in efficiency of fluorescence resonance energy transfer (FRET) between QDs and proximal organic dyes using a single excitation wavelength in order to discriminate ion sensitive emission signals. Co-immobilization of green emitting QDs with lucigenin, or valinomycin and a selected chromoionophore in acrylic nanospheres, resulted in Cl_2 sensitive and K^+ selective sensors, respectively. Embedding the resulting nanospheres in a polymeric matrix, dual sensitive ionic sensors with no cross-talk were created. In the presence of K^+ and Cl_2 the fluorescence of lucigenin was quenched, and QDs act as donors interacting with the deprotonated chromoionophore (acceptor) by FRET. As each ion was sensed by a different independent mechanism, the resulting luminescent response of the nanocomposite allowed monitoring the presence of each one of the analytes in different spectral regions in an independent manner.

Medintz and colleagues [135] used a related approach to develop a prototype FRET-based QD biosensor capable of measuring rates of enzymatic digestion. In their approach, peptides were synthesized to have domains specific for QD attachment, structural rigidity, protease recognition properties and dye labeling. In this initial state, fluorescence from the QD was significantly quenched by the dye. As an appropriate enzyme was added to solution some of the peptides were cleaved resulting in a substantial increase in fluorescence signal (dyes diffused away from the QD surface).

Authors indicated that by altering the recognition sequence (consisting of 2–4 selected amino acid residues) the "nanosensor" could be tuned to respond to a specific enzyme. Multifunctional QDs are also highly suited to sense more complex chemical species. In a relatively recent work, Potyrailo and co-workers [136] explored the use of different sized TOPO (tri-n-octylphosphine oxide) capped CdSe QDs incorporated into a polymer film. Upon photo activation, CdSe nanocrystals exhibited distinct photoluminescence response patterns when the film exposed to polar and non-polar vapors in air By using principal component analyses (PCA) of the spectral response of a multi QD doped film, a selective gas sensor was obtained, thus introducing the possibility of multi parameter gas sensing. The principle was demonstrated by exposing a PMMA (polymethylmetharcrylate) film doped with CdSe QDs (average sizes 2.8 nm and 5.6 nm diameter) to different concentrations of methanol and toluene. Results demonstrated that responses of the sensor film to the different vapors were well-separated in the PCA space, allowing for easy discrimination. This approach provides a complementary alternative to solvatochromic sensors based on chromo- and fluorescent dyes with benefits that include higher photo stability and sensitivity.

With purposely functional coatings, QDs are the "building blocks" for the assembly of new functionalities. So, the photoluminescence of quantum dots functionalized with molecularly imprinted polymers have been found to be a useful tool for the detection of small to medium sized analyte molecules [137,138]. While the MIP offers shape and selectivity, the QD responds by quenching the photoluminescence emission upon template binding. Lin et al. [138] applied MIP/QDs to the recognition and analysis of molecules of different size in urine real samples (creatinine, human serum albumin and lysozyme) and concluded that these multifunctional nanoparticles can be used not only to separate target molecules from biological fluids, but also to measure their concentrations in urine using low wavelength laser diode for the early detection of kidney dysfunction or inflammation.

In some cases, MIP/QD luminescence is enhanced upon template binding. Ersöz et al. [139] have developed MIP/CdS QDs against guanosine by immersing the nanocrystals in MAC (methacryloylamido-cysteine) in order to introduce methacryloyl groups onto the surface of CdS QDs. For the synthesis of the guanosine MIP nanoshell, the methacryloyl-activated nanocrystals were immersed in the pre-polymerization mixture containing a monomer/template metal-chelate, methacryloylamidohistidine-platinum-guanosine (MAH-Pt(II)/Gu). The guanosine can simultaneously bind to Pt(II) ion and fit into the shape-selective cavity. The binding affinity of the guanosine imprinted nanocrystals was investigated by using Langmuir and Scatchard methods. Experimental results demonstrated that MIP/CdS QDs selectively bound guanosine nucleotide ($K_a = 4.841 \times 10^6$ mol L^{-1}) and free guanine base ($K_a = 0.894 \times 10^6$ mol L^{-1}). Also, single stranded DNA fitted the multifunctional MIP/CdS QDs binding sites more favorably than double stranded DNA (Fig. 10).

Organic fluorescent dyes incorporated in MIP cavities have been used to report analyte binding [140] and quantum dots can also be used in a similar manner, but with a more stable sensitivity. A CdSe/ZnS quantum dot fixed with 4-vinyl-pyridine and a template (uracil and caffeine) were polymerized with ethylene glycol dimethacrylic acid as a cross-linker [141,142]. The quantum dots embedded in the polymers provided positive fluorescent responses after rebinding with the templates. In spite of the potential functionality, there have few published studies on MIP materials in conjugation with quantum dot probes.

Gamelin et al. [143] described in 2003 the synthesis and characterization of magnetic QDs based on ZnO doped with Co^{2+} and Ni^{2+}. Later, in 2005, Klimov et al. [144] developed the first all-inorganic core/shell hybrid magnetic-optical nanoparti-
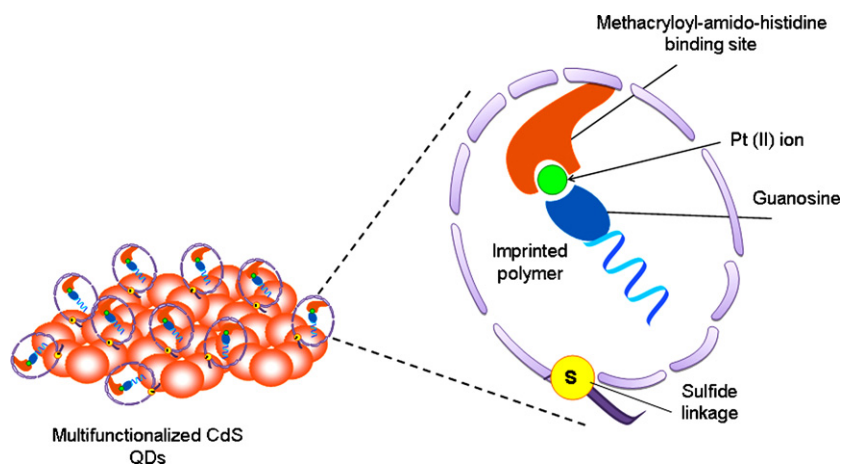
Fig. 10. Schematic representation of CdS QDs functionalized with molecularly imprinted sites against guanosine residues mediated by Pt (II) ions.

Table 2
Analytical applications of multifunctional quantum dots.

Surface linker	Attached moiety	Quantum dots	Analytical application	Ref.
TOPO + MES	–	CdSe	Free cyanide highly sensitive determination	[148]
Suitable amphiphilic Polymer	Streptavidin	CdSe/ZnS	Detection of E. Coli O157:H7 cells	[149]
Thioglycerol	–	CdS	Fe^{3+}, Cu^{2+}	[150]
Bovine serum albumin	–	CdSe/ZnS	Cu^{2+}	[151]
Terbutyl-N-(2-merccaptoethyl)carbamate	–	CdSe	Cyanide	[152]
TOPO	NIR luminescent squaraine dye	CdSe/ZnS	pH modulated FRET	[153]
Dithiolane anchoring group	[1,3]oxazine ligands	CdSe-ZnS	pH sensitive QD	[154]

TOPO: trioctyl-phosphine oxid.

cle, cobalt/cadmium selenide. The core/shell nanocrystals were prepared in a facile one-pot reaction by reacting at 140 °C Co nanoparticles with a solution of dimethylcadmium and Se-trioctylphosphine (TOP) complex dissolved in TOP, TOPO and n-hexadecylamine. No analytical prospects of these magnetic QDs were addressed; however, using magnetic and optical characterization, it was demonstrated a bifunctional behavior of the nanoparticles: the core retained the magnetic properties of the starting Co nanoparticle, and the shell emitted similarly to a single-component CdSe nanoparticle. This multifunctional QD is type vi, according to Gun'ko and colleagues classification [64]. It can be envisaged that synthesis and application of magnetic quantum dots, incorporated with different (bio)recognition molecules open a way for the fabrication of truly smart probes and (bio)chemical sensors, in high throughput detection and isolation of multiple target analytes, thereby greatly extending the usefulness of QDs.

Aside their already mentioned toxicity, QDs suffers from other drawbacks is that their photoluminescence fluctuate with time (also called blinking) [145]. Indeed, blinking may lower the effective quantum efficiency and thereby degrade the performance of devices (e.g. sensors) designed with QD active elements, especially those containing only a few QDs. Despite over a decade of research, completely non-blinking QDs have not been synthesized. Only recently, it has been reported semiconductor nanocrystals that individually exhibit continuous, non-blinking photoluminescence: these non-blinking nanocrystals may enable substantial advances in fields ranging from single-molecule biological labelling to low-threshold lasers [146,147].

In Table 2 the functionalization of QDs with different linkers and (bio)molecules necessary for different sensing applications are summarized, while in previous sections, examples of multifunctional hybrid nanoparticles made of AuNPs/QDs and MNPs/QDs have already been considered.

5. Multifunctional carbon and inorganic nanotubes

A major barrier for developing practical carbon nanotube (CNT) analytical approaches is the insolubility of carbon nanotubes in most solvents. Their manipulation and processability is highly desired to broaden the great potential of application of CNTs-based sensing devices. Surface functionalization of carbon nanotubes is an effective way of improving the solubility and dispersion of the nanotubes in aqueous solutions and to design new hybrid materials by coupling the properties the functional layers to those of carbon nanotubes [155–158]. Some drawbacks of carbon nanotubes as low material processing control (purification, chirality and debundling).

An excellent review about the applications of functionalized CNTs for biosensing has been recently published by Wang and Li [159]. The review summarizes recent advances in electrochemical biosensors based on carbon nanotubes (CNTs) and carbon nanofibers (CNFs) with an emphasis on applications of CNTs and a few references devoted to analytical applications of multifunctional CNTs. Another interesting review by Rao et al. [160] gives a concise account of CNTs and the use of carbon nanotubes as sensors followed by detailed account on need and subsequent virtues on functionalization/grafting of CNTs with various species, highlighting the functionalization/grafting of DNA onto single wall carbon nanotubes (SWCNTs) and multi wall carbon nanotubes (MWCNTs) for developing biosensors for selective recognition of DNA. The attachment of metal nanoparticles, particularly Au nanoparticles, to functionalized carbon nanotubes has recently been an active field of research for gas-sensor and catalytic applications [161–165].

Some of these multifunctional CNTs with analytical potential have been reported along the last few years. In 2007, Gogotsi et al. [166] described the synthesis of multifunctional CNTs with gold or iron oxide nanoparticles and their potential use for sensing glycine. The nanotube synthesis process was performed using the well known non-catalytic carbon vapor deposition (CVD) template-
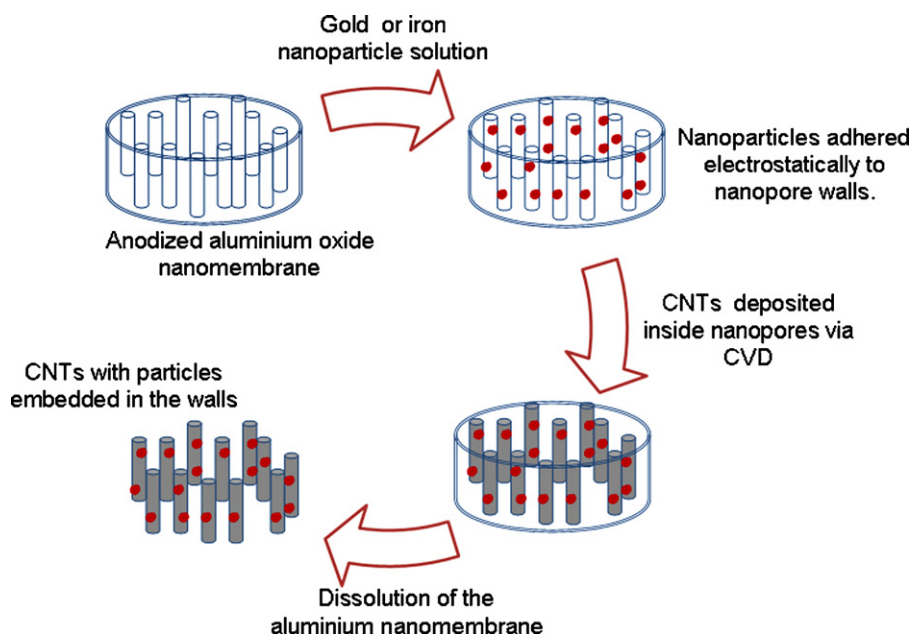
Fig. 11. Template synthesis of functionalized carbon nanotubes with AuNPs or iron nanoparticles.

assisted approach [167]. Anodized aluminum oxide membranes (with pore diameters ranging from 20 to 200 nm and with lengths up to 90 μm) were used as templates for CNT growth. These membranes were immersed in acidic solutions containing the corresponding Au or iron nanoparticles which adhered electrostatically to the template walls. Then nanotubes were then deposited inside the membrane pores via CVD. Dissolution of the aluminum nanomembrane in boiling NaOH left behind CNTs with particles embedded in the walls (Fig. 11).

Incorporation of particles produced plasmon resonance and allowed surface enhanced Raman spectroscopy studies with single-molecule sensitivity. Experimental results demonstrated that Raman spectra of CVD carbon nanotubes with and without Au nanoparticles showed no significant difference. However, it was interesting to observe that while addition of CNTs without Au particles to a glycine solution yielded no Raman signal changes, signal enhancements were achieved only with nanotubes with gold particles embedded in the walls. Authors explained this enhancement suggesting that the surface-enhanced Raman scattering (SERS) signal for glycine was due uniquely to glycine molecules close to the Au nanoparticles, which were mainly inside the nanotube. The concentration of glycine in the solution was too low to be observed by the conventional Raman technique and, consequently, glycine outside the nanotube cannot yield any signal. Comparison of these results to SERS of glycine in an Au colloid solution showed an up shift of about 5–10 cm^{-1} of the glycine peaks, possibly due to the presence of the carbon layer between the gold and the glycine. Authors highlighted that these results open the way to the development of nanotube based SERS probes for the detection of extremely small amounts of biological and chemical components dispersed in liquids or cellular research. On the other hand, application of CNTs functionalized with magnetic nanoparticles was not analytically assayed. However, Gogotsi et al. [166] claimed that a key advantage of the CNTs modified with magnetic nanoparticles was that the cavity of the CNT was empty and that fact could allow CNT alignment in the presence of a magnetic field without interfering with fluid flow inside the CNTs. These magnetically active tubes could also be manipulated through magnetic assembly in micro- and nanodevices or loaded with drugs, driven to a specific location inside a cell or used for biosensing. In the magnetic nanotubes syn-

thesized in their work, metal particles were always covered by a carbon layer which did not allow direct chemical reaction or loss of particles in the environment.

A combination of MWCNTs, cobalt porphyrin and tungsten oxide in the film (deposited onto glassy carbon electrode substrate) has been recently described by Kulesza et al. [168]. Such combination produced an electrocatalytic system capable of effective reduction of oxygen in acid medium (0.5 mol L^{-1} H$_2$SO$_4$). The simultaneous presence of cobalt porphyrin and tungsten oxide, together with dispersed carbon nanotubes, led to an enhancement effect evident from positive shifting in the oxygen reduction voltammetric potential and a significant increase of voltammetric currents (relative to those characteristic of the system free of carbon nanotubes and WO$_3$). The multi-component electrocatalytic film also exhibited relatively higher activity towards reduction of hydrogen peroxide. Authors suggested that the reduction of oxygen was initiated at the cobalt porphyrin redox centres, and the undesirable hydrogen peroxide intermediate was further reduced at the tungsten oxide support. An important function of carbon nanotubes was to improve transport of electrons within the electrocatalytic multi-component film. Although authors recognized that the performance of Co-porphyrin/WO$_3$/CNTs catalyst was lower in comparison to Pt-based systems, their system was largely ethanol tolerant, a fact of particular importance where highly selective cathode electrocatalysts were required such as in applications in fuel cells utilizing alcohols.

The synthesis and characterization of several hybrid [60]fullerene/SWCNT materials that combine [60] fullerenes with appended photoactive ferrocenyl or porphyrinyl functionalities and SWCNTs into a single multifunctional structure have been described by Bonifazi and co-workers [169]. In this structure, the dyads were covalently attached to the exo-surface of SWCNTs. The presence of the porphyrinyl and ferrocenyl fragments acted as effective chromophores and electroactive species, respectively. Authors concluded that more work was needed in order to determine the potential properties of these novel hybrid materials in the design of functionalized WCNTs, not only for photovoltaic or optoelectronic applications, but also for medical and bio-applications; for example, in the field of diagnosis and treatment by simply linking molecular modules that contain Gd(III) ions.
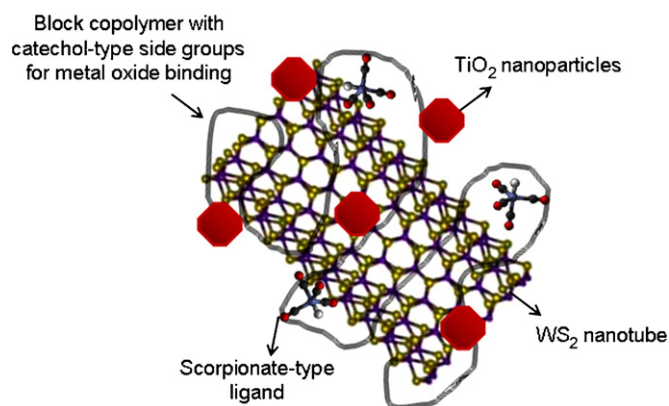
Fig. 12. Multifunctional WS nanotubes. Adapted from Ref. [179].

Inorganic oxide nanotubes can be also functionalized by using molecular surface linkages based on siloxane [170–172], carboxylic acid [173], acetyl acetonate [174], phosphonate [175–177] or catecholate [178,179] functional groups. While covalent functionalization of inorganic oxide nanotubes is a relatively easy task, layered chalcogenides are much more inert because of the sulphur lone electron pairs pointing away from the surfaces, while the metal is sandwiched by the chalcogen layers and, therefore, hardly accessible for complexation by any ligands. In fact, papers devoted to chalcogenide nanotubes functionalization are practically lacking. Tremel et al. [180] reported the first chemically specific and facile method for the functionalization of WS_2 nanotubes and the subsequent coating of the functionalized WS_2 nanotubes with monocrystalline TiO_2 (anatase) nanoparticles by using a multifunctional polymeric ligand that had three different functional groups: (1) a nitrilotriacetic acid (NTA) linker used to coordinate to Ni^{2+} ions which, in turn, provided vacant coordination sites for binding to the surface S atoms of WS_2 nanotubes, (2) an anchor group for attachment onto the surface of metal oxide nanoparticles (TiO_2, ZrO_2, Fe_2O_3, etc.) and (3) a fluorescent dye molecule for detection purposes. They carried out functionalization and coating of WS_2 nanotubes with TiO_2 nanoparticles by anchoring of the organic ligand to the sulphur surface by using the Ni^{2+} ion as a soft transition metal, whose octahedral coordination sphere was blocked completely on one side by the scorpionate-type ligand (NTA) while the other part of the coordination sphere remained vacant for binding to the surface S atoms of WS_2 nanotubes. Then, immobilization of TiO_2 nanoparticles was performed by using free catecholate groups (3-hydroxytyramine), as shown in Fig. 12. As the reaction in the absence of Ni^{2+} ions did not show binding of the polymeric lig-

and to the WS_2 nanotubes, authors concluded that the Ni^{2+} ions were involved in the binding of the multifunctional polymer to the chalcogenide nanotube. Due to their exceptional mechanical properties, authors suggested that functionalization of WS_2 nanotubes opens several new fields for this class of materials, fields that have been pursued actively during the past few years for the related carbon nanotubes and various oxide materials [180].

Zhang and Zhao [181] also described a nanocrystal self-assembly method for the preparation of rare earth fluoride nanotubes (REF-NTs) arrays and magnetite-doped rare earth fluoride nanotubes (Fe_3O_4 REF-NTs) by using porous anodic aluminum oxide (AAO) as hard template. The REF-NTs were prepared by the impregnation of α-$NaYF_4$ nanocrystals doped with Yb^{3+} and Er^{3+} into the porous of an AAO membrane (Fig. 13). Scanning electron microscopy (SEM) and transmission electron microscopy (TEM) images demonstrated that the nanotubes were composed of close-packed uniform nanocrystals. Similarly, the Fe_3O_4 REF-NTs were obtained by the self-assembly of a mixture of Fe_3O_4 and Yb/Er doped β-$NaYF_4$ nanocrystals in the AAO pore channels. Strong up-conversion fluorescent emissions were realized for the nanotube arrays and multifunctional nanotubes with up-conversion excitation in the near-infrared (NIR) region. A strong magnetic response of the multifunctional nanotubes was observed, which facilitated their separation from solution by magnetic decantation using a permanent magnet. Although no analytical application has been performed with these multifunctional nanotubes, authors suggested that by combining the attractive tubular structure with up-conversion fluorescent and magnetic properties, the resulting multifunctional nanotubes are ideal candidates for biomedical applications such as bioseparation and targeted drug delivery.

6. Other multifunctional nanoparticles

6.1. Silica nanoparticles

Silica is a very appealing material for analytical applications because it is relatively inexpensive, chemically inert, thermally stable, and biocompatible. In fact, silica nanoparticles have gained much attention over the past two decades for their application in catalysis, separation, (bio)sensors, and adsorption. There are several properties that make silica nanoparticles attractive as analytical materials [182,183]. Particle sizes can be tuned from 50 to 300 nm, with stable and rigid frame that allows for resistance to mechanical stress and degradation. Pore diameters can be tuned between 2 and 10 nm allowing for different chemicals/analytes loadings. Also, they have a high surface area (>700 m^2/g) and large pore volume (>0.9 cm^3/g) allowing high loadings of chemicals. Sil-
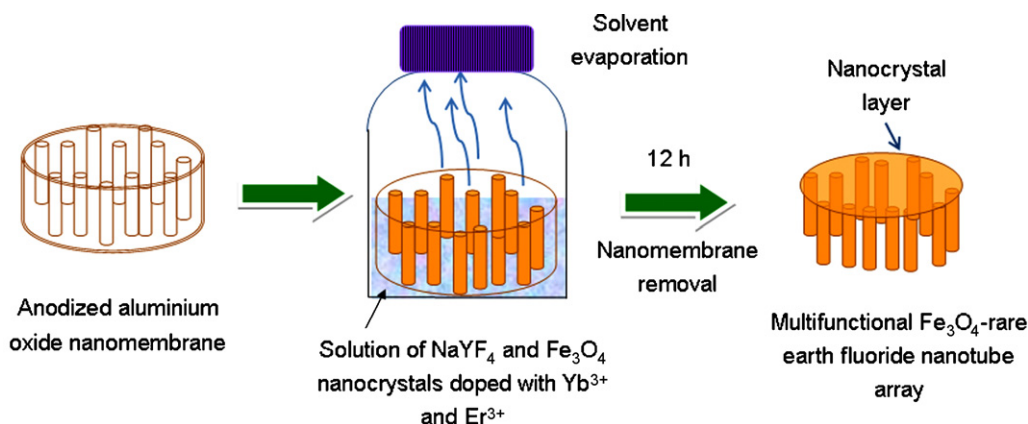

Fig. 13. Development of a multifunctional Fe_3O_4 rare earth fluoride nanotube array.
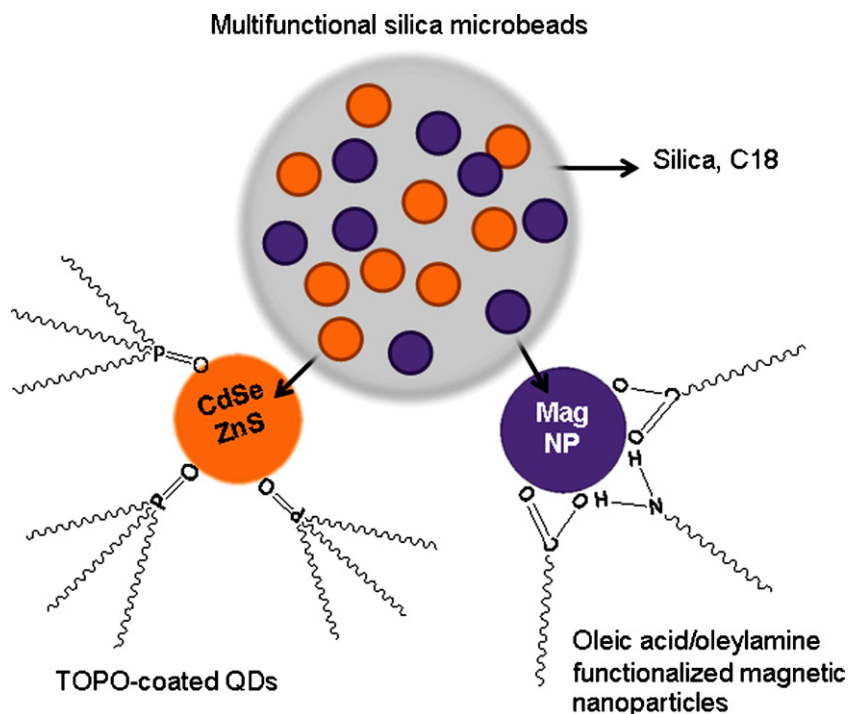
Multifunctional silica microbeads

Fig. 14. Scheme illustrating the internal structure of dual-function optical and magnetic mesoporous silica beads. TOPO: Trioctylphosphine Oxide.

ica nanomaterials are "transparent". Also, silica sols in the size range of 10–100 nm have been observed to possess a remarkable stability at very high salt concentrations (e.g., 0.15 M NaCl) at pH > 10.5 [184,185] and even at their isoelectric point (pH_{iep}) [186]. They are unlikely to absorb light in the near-infrared, visible and ultraviolet regions or to interfere with magnetic fields, which allows dopants/functional groups inside silica matrix to keep their original optical and magnetic properties. Consequently, the interior and exterior surfaces of silica nanoparticles can be selectively functionalized with different moieties on either surface [182,183].

Silica nanoparticles are relatively easy to be prepared by Stöber method [187] that involves the hydrolysis and condensation of TEOS in ethanol solution in the presence of water with ammonia as a catalyst to create monodisperse, spherical, electrostatically stabilized particles. Alternatively, spherical silica nanoparticles can also be made by reverse micro emulsion [188] a technique that relies on the controlled aqueous environment within surfactant-confined micelles in a non-polar solvent to create monodisperse spherical colloids.

Multifunctional silica mesoporous particles were developed by Nie et al. [189]. They developed silica micro beads embedded with both semiconductor quantum dots (QD) and iron oxide (Fe_3O_4) nanocrystals as a new class of dual-function carriers for optical encoding and magnetic separation (Fig. 14). Silica beads derivatized with C18 alkyl chains were used as they offered a strongly hydrophobic environment for the incorporation of tri-n-octylphosphine oxide-coated QDs and oleic acid/oleylamine coated-iron oxide nanoparticles. The embedding (doping) process was carried out by either simultaneous or sequential addition of quantum dots and iron oxide (Fe_3O_4) nanocrystals to a well-mixed solution silica beads dissolved in butanol. Due to the highly porous internal structure and very large surface area, the mesoporous beads (with pore sizes ranging from 2 to 100 nm) allowed up to 1 million nanoparticles to be incorporated into a single micrometer-sized bead. Iron oxide nanocrystals provided superparamagnetic properties for bead separation and target enrichment, although they attenuated the QD fluorescence intensity not by a typical

quenching process but as result of the broad optical absorption spectrum of mixed-valence Fe_3O_4. In order to improve biocompatibility and reduced non-specific binding, the encoded beads were further coated with amphiphilic polymers such as octylaminepoly (acrylic acid). The results indicate that the polymer-coated beads were well-suited for target capturing and enrichment, yielding magnetic separation efficiencies higher than 99%. By using beads doped with QDs emitting in the green and red wavelengths, authors demonstrated that it was possible to prepare dual-function optical and magnetic beads encoded with three different and discernible spectroscopic signatures. These encoded beads are expected to find broad applications in high-throughput and multiplexed biomolecular assays.

More recently, Gao et al. [190] have described an ultrasensitive detection of 2,4,6-trinitrotoluene (TNT) based on fluorescence quenching of a fluorescent silica nanoparticle. In their approach silica nanoparticles were first modified with amine groups using APTS and then, a fluorophore (5(6)-fluorescein isothiocyanate (FITC) or 6-carboxy-X-rhodamine N-succinimidyl ester (ROX))was immobilized on the silica nanoparticle surface. TNT bound to the amine group on the nanoparticle surface and absorbed energy from the nearby FITC via fluorescence energy transfer. This process resulted in quenching of the dye fluorescence signal. The detection limit reached 1 nM TNT in solution and several ppb of TNT vapor in air. By a similar method, Pb^{2+} and Ni^{2+} ions were determined [191,192]. Recent progress in silica NP research, with special emphasis on applications in the fields of bio-labeling, imaging, separation, analysis, disease diagnostics and therapeutics, and other related technologies has been recently reviewed [182,183]. Silica nanoparticle synthesis and (bio)functionalization were also discussed in these works.

6.2. TiO₂ nanoparticles

TiO_2 exists in several crystalline modifications, being the most common forms anatase and rutile. TiO_2 nanoparticles have been attracting a great deal of attention due to their potential appli-

cations for the development of solar cells and photocatalysts for sterilization in food and the environmental industry, as well as in water and air purification [193,194]. These applications are based on generation of photoinduced electrons and holes on the conduction and valence bands when TiO_2 absorbs ultraviolet-A light (320–400 nm) with a wavelength less than 385 nm (or energy greater than the band gap of TiO_2).

Microemulsion methods have used to prepare TiO_2 nanoparticles [195–197]. Reverse micelles provide a cage-like effect that can control nucleation, growth and agglomeration. On the other hand, the possibility to vary the size of the micellar core, by simply altering the water to surfactant ratio, provides a very convenient handle to control the particle sizes. Recently, a "microscopic mass point addition" method has been developed to fabricate high density TiO_2 nanodots with controllable size on a Si substrate. In this approach an alumina filtration membrane with homogenous micropores acted as the "microscopic mass point" nozzle [198]. Authors claimed that these TiO_2 nanodots deserve potential to be used as optical devices, high performance sensor and highly active catalysts.

TiO_2 nanoparticles have been also prepared by the sol–gel technology [199–203]. These nanoparticles are amorphous in nature and need further heat treatment to get a crystalline product [204]. For the synthesis of anatase TiO_2 nanocrystallites, much attention has been paid to hydrothermal methods [205–207], in which the chemical reaction can proceed under auto-generated pressure upon heating. The process is efficient enough to achieve the crystalline phase at relatively low temperatures and the particles prepared through hydrothermal synthesis are expected to have large surface area, smaller crystallite size, and higher stability than those obtained by other methods such as the sol–gel technology or the microemulsion processes. The hydrothermal method has also been used to prepare TiO_2 nanotubes [208,209]. The solvothermal method, a powerful route for preparing nanomaterials of oxides and metal chalcogenides, is similar to the hydrothermal method except that organic solvents are used instead of water [210–211]. In this approach chemical reactions take place in an organic solvent under supercritical or sub-critical pressures under different temperature conditions. Solvothermal process provides an excellent chemical homogeneity and the possibility of synthesizing meta-stable structures with different morphologies at low-reaction temperatures [211–213].

Compared to SiO_2 nanoparticles or to conventional quantum dots, there is virtually no analytical work using multifunctional TiO_2 nanoparticles; even, work using raw or monofunctional TiO_2 nanoparticles, is scarce. Some work, in combination with other nanoparticles has been recently published. Yuan et al. [214] have prepared on a gold electrode a multifunctional film based on highly hydrophilic, non-toxic and conductive TiO_2 nanoparticles/gold nanoparticles bilayer. Subsequently, positively charged horseradish peroxidase (HRP) was assembled onto the bilayer films, which provided an interface to assemble gold nanoparticles for immobilization of carcinoembryonic antibody (anti-CEA). Finally, HRP was used to block sites against non-specific binding. Electrochemical impedance spectroscopy (EIS) and cyclic voltammetry (CV) were applied to characterize the electrochemical properties of the self-assembly process. The CVs reduction current of the immunosensor decreased linearly in two concentrations ranges of CEA from 0.3 to 10 ng mL^{-1} and from 10 to 80 ng mL^{-1} with a detection limit of 0.2 ng mL^{-1} in presence of 0.7 mM H_2O_2 in analyte solution. The proposed immunosensor exhibited good accuracy, high sensitivity, long-term stability and made it to determine CEA in serum samples with satisfactory results. The multifunctional nanocomposite matrix showed good hydrophilicity and was effective for tunneling electrons between immobilized HRP and electrode surface and for retaining the bioactivity of immobilized

molecules. According to the authors, the developed protocol has several attractive advantages including simple fabrication, long-time storage stability, high sensitivity, and it could be extended to the determination of other species of clinical or environmental concern.

Llobet and colleagues [215] have prepared hybrid titania films using a modified sol–gel route for obtaining well-dispersed hydrogen plasma-treated multiwall carbon nanotubes in either pure titania or Nb doped titania for oxygen sensing. Oxygen responsiveness of Nb doped TiO_2/CNT materials outperformed that of Nb doped titania, although it was lower than that of TiO_2/CNT samples. Authors explained this fact considering that presence of CNTs could alter the optimal value for the concentration of Nb in TiO_2. The gas sensitivity studies performed on the different samples have shown that the hybrid layers based on titania and carbon nanotubes possess an unprecedented responsiveness towards oxygen (i.e. more than four times higher than that shown by optimized Nb doped TiO_2 films). According to the authors, these new hybrid sensors show a strong potential for monitoring traces of oxygen (i.e. ≤10 ppm) in a flow of CO_2, which is interesting for the beverage industry.

More recently, Cai et al. [216] have prepared carbon nanotubes (CNTs)-modified titania nanotube (NT) arrays by vapor-growing CNTs in the inner of titania NTs. Pt nanoparticles of ~3 nm in diameter were uniformly decorated on the as synthesized titania-supported CNTs (TiO_2/CNTs) electrode, showing remarkably improved catalytic activities for the oxidation of hydrogen peroxide. The glucose biosensor fabricated by modifying TiO_2/CNT/Pt electrode with glucose oxidase (GOx) presented a high sensitivity of 0.24 μA mM^{-1} cm^{-2} to glucose in the range of 0.006 mM to 1.5 mM with a response time of less than 3 s and a detection limit of 5.7 μM at 3 signal/noise ratio. The success of the biosensor was ascribed to the large surface area and good conductivity of CNT network, the highly dispersed Pt nanoparticles, and the excellent biocompatibility of TiO_2 to H_2O_2.

Although much attention has been paid to the synthesis of TiO2 nanoparticles, their potential applications in analytical chemistry have been scarcely studied despite the expectation that nanoparticles have in analytical nanotechnology.

6.3. Gadolinium nanoparticles

Gd_2O_3 nanoparticles constitute an excellent host matrix for the luminescent rare-earth ions such as Tb^{3+}. Nanosized gadolinium oxide nanoparticles, doped by luminescent rare earth ions, result in highly photostable luminescent nanoparticles characterized by narrow emission bands [217–220]. A polysiloxane shell (APTEOS and TEOS) ensured not only the protection of the core and favours the dispersion of the nanoparticles in aqueous solution without loss of luminescence of rare earth ions, but also an amplification of luminescence attributed to the replacement of Tb-OH surface groups (detrimental for luminescence) by Tb-O-Si groups and to an energy transfer from polysiloxane shell to Tb^{3+} ions [221]. Besides these actions, the polysiloxane shell facilitated, thanks to the presence of amine functions of APTEOS, the functionalization of the particles with different types of molecules without prejudicial competition.

Although the physical properties of lanthanide oxide nanoparticles have been extensively studied, there are only a few reports dealing with their analytical applications [222,223]. As an example, to overcome photo bleaching and spectral overlapping observed when dyes are used as labels in immunoassay microarrays, Kennedy et al. [223] developed a new type of fluorophore based on crystalline europium-doped gadolinium oxide (Eu:Gd_2O_3) nanoparticles. The synthesized Eu:Gd_2O_3 nanoparticles exhibited narrow red emission, large Stokes shift, photostable laser-induced fluorescence with a long lifetime (1 ms). In order to covalently conjugate antibodies, amino functionalization of the

particles was achieved by poly (l-lysine) (PL) encapsulation. The multifunctional nanoparticles were then successfully applied as reporters in a competitive fluorescence micro immunoassay for phenoxybenzoic acid (PBA), a generic biomarker of human exposure to pyrethroid insecticides. Microarrays were fabricated by micro contact printing of BSA–PBA in line patterns ($10 \times 10\,\mu m$). The microarray immunoassay demonstrated a limit of detection of $1.4\,\mu g\,L^{-1}$ PBA. The results of this research offer potential applications of lanthanide oxide nanoparticles as fluorescent probes in microarray and biosensor technology, immunodiagnostics, and high-throughput screening.

For benefiting of the promising properties of Gd_2O_3 nanoparticles for biological detection, Tillement et al. [224] synthesized doubly luminescent core/shell structure nanoparticles: firstly, gadolinium oxide (Gd_2O_3) core was doped with the luminescent Tb^{3+} ions in a polyalcohol medium. As water is a strong quencher of terbium ion's luminescence, Gd_2O_3-Tb^{3+} nanoparticles were embedded in a functionalized polysiloxane shell prepared by hydrolysis condensation of a mixture of APTEOS and TEOS. This protective layer allowed the dispersion of the particles in aqueous solution with the advantage that the luminescence intensity of polysiloxane coated Gd_2O_3 nanoparticles was greatly enhanced compared with the naked Gd_2O_3 core. Due to the presence of amino groups, organic dyes and bio targeting groups (nucleic acid, biotin, streptavidin) were covalently linked to the polysiloxane network. These particles were efficient for detection of bio molecules whose presence was revealed by the high fluorescence of organic dyes and/or the photostable Tb^{3+} ion's luminescence.

Literature on lanthanide-doped nanoparticles is explosively growing and in a recent review [225], different types of lanthanide-based hybrid materials (including nanoparticle lanthanide ion-doped inorganic sol–gel glasses and polymers doped with organic lanthanide complexes) are described, comparing their respective advantages and disadvantages as well as their applications.

7. Conclusions

Nanomaterials offer unique opportunities for designing ultrasensitive (bio)sensors and analytical assays. This review demonstrates the broad potential of multifunctional nanoparticles for (bio)molecular recognition events and separations. We have selected some of the outstanding examples from the literature where the special features of typical multifunctional nanoparticles are partially or fully utilized to outstanding effect. The remarkable sensitivity of the new multifunctional nanoparticle-based sensing protocols opens up the possibility for detecting disease markers, biothreat agents, chemicals or infectious agents that cannot be measured by conventional methods. The use of multifunctional nanoparticles for detecting proteins is still in its infancy (most of the work has been focused on separations), but the experience gained in ultrasensitive DNA detection may provide a useful starting point. Despite analytical research in the field is active there is still much space to explore and to explain, tremendous opportunities and significant challenges to be afforded. For example, whereas present work is more concentrated on multifunctional magnetic nanoparticles, very few studies on multifunctional gold nanoparticles or QDs are still appearing. Probably the most prominent advantage of multifunctional magnetic nanoparticles over others lies in the fact that the particles can be easily functionalized and magnetically manipulated using permanent magnets independent of normal chemical or biological analysis.

The challenges of processing nanoparticles easily and their multifunctionalization with (bio)molecules or other nanoparticles in a biological and chemical friendly manner are just beginning to be addressed. Just starting with the base nanoparticle, one of the most significant barriers along the road is the poor reproducibility and the wide range of size distribution of nanoparticle product synthesized from wet chemical methods. Improved synthetic methodologies that can lead to true monodispersity and satisfactory reproducibility of nanoparticles with well-controlled shape remain to be developed. On the other hand, nanoparticle surface modification is also a critical step for protecting the nanoparticle core, improving aqueous dispersibility, and obtaining appropriate surface multifunctionality for the development of highly sensitive and selective "nanosensors". Even, from a physic-chemical point of view, clear and quantitative characterizations of the surface chemistry of the nanoparticles should be provided in terms of the number of surface reactive functions that are effectively present at the surface of the particles. From literature surveys so far, virtually no analytical studies have been dedicated to multifunctional silica, -titania, -inorganic nanotubes, etc., and it should be another potential aspect in research.

The rapid advancement of imaging technology over the past decade has opened opportunities for the design of specific and multifunctional nanoprobes for medical and pharmaceutical applications such as molecular imaging, drug delivery, targeting and cancer research, some of which can be considered analytical in nature [226–230]. The use of multifunctional nanoparticles would have advantage for pre-operative tumor assessment and intraoperative surgical guidance for the tumor tissue resection. Whereas successful experiments were conducted *in vitro*, progress in practical applications of these multifunctional nanoparticles may be slow, particularly due to the unknown effects of nanoparticles in human health [231–233].

We hope to have shown that this novel area of applications of multifunctional nanoparticles offers many exciting possibilities for future developments. The development of novel multifunctional nanomaterials and the exact investigation of their performance characteristics open the way to new analytical devices in the future. It is a highly multidisciplinary area, requiring a range of scientific knowledge, from inorganic/organic chemistry involved in the preparation of different types of nanoparticles, through chemistry and biological sciences to allow for their functionalization and, of course, the basic physics of optics and magnetic materials. It is now generally recognized that nanotechnologies and biosciences will be one of the leading and most promising areas of research and development in the 21st century. We believe that multifunctional nanoparticles could play a very important role in these developments.

Acknowledgments

References

[1] Nanomaterials Handbook; Ed. Yury Gogotsi; ISBN: 9780849323089, CRC Taylor and Francis, Boca Ratón, FL, 2006.
[2] Nanochemistry. A chemical approach to nanomaterials; Geoffrey A. Ozin, André C. Arsenault; RSC Publishing, Cambridge (UK), 2005.
[3] Nanoparticles: building blocks for nanotechnology (Series: Nanostructure Science and Technology) Vincent Rotello; ISBN: 978-0-306-48287-8, Springer, 2004.
[4] K.L. Kelly, E. Coronado, L.L. Zhao, G.C. Schatz, J. Phys. Chem. B 107 (2003) 668.
[5] P. Alivisatos, Pure Appl. Chem. 72 (2000) 1.
[6] M.J. Green, Na. Behabtu, M. Pasquali, W.W. Adams, Polymer 50 (2009) 4979.
[7] Q. Huo, Colloids Surf. B: Biointerfaces 59 (2007) 1.

[8] G. Han, P. Ghosh, V.M. Rotello, Multifunctional gold nanoparticles for drug delivey; Bio-Applications of Nanoparticles, Chapter 4; Ed. Warren C.W. Chan; Landes Bioscience and Springer Science + Business Media, 2007.
[9] J. Kim, J.E. Lee, J. Lee, Y. Jang, S.W. Kim, K. An, J.H. Yu, T. Hyeon, Angew. Chem. Intern. Ed. 45 (2009) 4789.
[10] A.S. Teja, P.Y. Koh, Prog. Cryst. Growth Charact. Mater. 55 (2009) 22.
[11] I. Koh, L. Josephson, Sensors 9 (2009) 8130.
[12] X.M. Lin, A.C.S. Samia, J. Magn. Magn. Mater. 305 (2006) 100.
[13] S. Qadri, A. Ganoe, Y. Haik, J. Hazard. Mater. 169 (2009) 318.
[14] Q. Yuan, R.A. Williams, China Particuol. 5 (2007) 26.
[15] W. Wu, Q. He, C. Jiang, Nanoscale Res. Lett. 3 (2008) 397.
[16] M. Alejandro-Arellano, A. Blanco, T. Ung, P. Mulvaney, L.M. Liz-Marzán, Pure Appl. Chem. 72 (2000) 257.
[17] B. Arkles, Chemtechnology 7 (1977) 766.
[18] H. Xu, N. Tong, L. Cui, Y. Lu, H. Gu, J. Magn. Magn. Mater. 311 (2007) 125.
[19] H. Tian, J. Li, Q. Shen, H. Wang, Z. Hao, L. Zou, Q. Hu, J. Hazard Mater. 171 (2009) 459.
[20] P.K. Jal, M. Sudarshan, A. Saha, S. Patel, B.K. Mishra, Colloids Surf. A: Physicochem. Eng. Aspects 240 (2004) 173.
[21] P.K. Jal, S. Patel, B.K. Mishra, Talanta 62 (2004) 1005.
[22] M. Yan, O. Ramström (Eds.), Molecularly Imprinted Materials, Marcel Dekker, New York, 2005.
[23] B. Sellergren (Ed.), Molecularly Imprinted Polymers, Man-Made Mimics of Antibodies and their Application in Analytical Chemistry, Elsevier, UK, 2000.
[24] M. Komiyama, T. Takeuchi, T. Mukawa, H. Asanuma, Molecular Imprinting: From Fundamentals to Applications, Wiley-VCH, 2003.
[25] R.J. Ansell, K. Mosbach, Analyst 123 (1998) 1611.
[26] Y. Ji, J. Yin, Z. Xu, C. Zhao, H. Huang, H. Zhang, C. Wang, Anal. Bioanal. Chem. 395 (2009) 1125.
[27] X. Wang, L. Wang, X. He, Y. Zhang, L. Chen, Talanta 78 (2009) 327.
[28] X. Kan, Z. Geng, Y. Zhao, Z. Wang, J.-J. Zhu, Nanotech. 20 (2009) 165601.
[29] Y. Li, X.-F. Yin, F.-R. Chen, H.-H. Yang, Z.-X. Zhuang, X.-R. Wang, Macromolecules 39 (2006) 4497.
[30] J. Szejtli, Chem. Rev. 98 (1998) 1743.
[31] K.A. Connors, Chem. Rev. 97 (1997) 1325.
[32] T. Cserhati, E. Forgacs, Cyclodextrins in Chromatography; RSC Chromatography Monographs, in: Roger M. Smith (Ed.) Cambridge, UK, 2003.
[33] Y. Wu, F. Zuo, Z. Zheng, X. Ding, Y. Peng, Nanoscale Res. Lett. 4 (2009) 738.
[34] Y.B. Sun, X.B. Ding, Z.H. Zheng, X. Cheng, X.H. Hu, Y.X. Peng, Eur. Polym. J. 43 (2007) 762.
[35] Avidin–Biotin Technical Handbook; Thermo Fisher Scientific Inc., 2009.
[36] Methods in Molecular Biology. Avidin-biotin Interactions: Methods and Applications, in: McMahon, R.J. Springer (Ed.), 2008.
[37] E.A. Bayer, M. Wilchek, Meth. Biochem. Anal. 26 (1980) 1.
[38] I. Hafaid, A. Gallouz, W.M. Hassen, A. Abdelghani, Z.Sassi, F. Bessueille, N. Jaffrezic-Renault, J. Sensors, Vol. 2009, (2009) Article ID 746548.
[39] A. Erdem, F. Sayar, H. Karadeniz, G. Guven, M. Ozsoz, E. Piskin, Electroanalysis 19 (2007) 798.
[40] R. Narain, M. Gonzales, A.S. Hoffman, P.S. Stayton, K.M. Krishnan, Langmuir 23 (2007) 6299.
[41] G. Decher, Science 277 (1997) 1232.
[42] H.C. Yoon, M.Y. Hong, H.S. Kim, Anal. Chem. 72 (2000) 4420.
[43] W. Yang, J. Wang, S. Zhao, Y. Sun, C. Sun, Electrochem. Commun. 8 (2006) 665.
[44] F. Ricci, G. Palleschi, Biosens. Bioelectron. 21 (2005) 389.
[45] M. Florescu, C.M.A. Brett, Anal. Lett. 37 (2004) 871.
[46] J.A. Hansen, J. Wang, A.N. Kawde, Y. Xiang, K.V. Gothelf, G. Collins, J. Am. Chem. Soc. 128 (2006) 228.
[47] C.W. Hunga, T.R.P. Holoman, P. Kofinas, W.E. Bentley, Biochem. Eng. J. 38 (2008) 164.
[48] J. Li, X. Wei, Y. Yuan, Sen. Actuator B 139 (2009) 400.
[49] Z. Liu, Y. Liu, H. Yang, Y. Yang, G. Shen, R. Yu, Anal. Chim. Acta 533 (2005) 3.
[50] G.K. Kouassi, J. Irudayaraj, G. McCarty, J. Nanobiotech. 3 (2005), doi:10.1186/1477-3155-3-1.
[51] D. Tang, J.C. Sauceda, Z. Lin, S. Ott, E. Basova, I. Goryacheva, S. Biselli, J. Lin, R. Niessner, D. Knopp, Biosen. Bioelectron. 25 (2009) 514.
[52] A. del Campo, T. Sena, J.P. Lellouchec, I.J. Bruce, J. Magn. Magn. Mater. 293 (2005) 33.
[53] D. Tang, Z. Zhong, R. Niessner, D. Knopp, The Analyst 134 (2009) 1509.
[54] L. Li, X.W. He, L.X. Chen, Y.K. Zhang, Sci. China Series B: Chem. 52 (2009) 1402.
[55] Y. Ren, X. Wei, M. Zhang, J. Hazard. Mater. 158 (2008) 14.
[56] C. Huang, B. Hu, Spectrochim. Acta Part B 63 (2008) 437.
[57] H. Cao, J. He, L. Deng, X. Gao, Appl. Surf. Sci. 255 (2009) 7974.
[58] E. Heim, F. Ludwig, M. Schilling, J. Magn. Magn. Mater. 321 (2009) 1628.
[59] S.V. Sonti, A. Bose, Colloid Surf. B: Biointerf. 8 (1997) 199.
[60] J.H. Jang, H.B. Lim, Microchem. J. 94 (2010) 148.
[61] Q. Cheng, T.Z. Peng, A.L. Liu, Chin. Chem. Lett. 16 (2005) 1059.
[62] D. Tang, H. Li, J. Liao, Chem. Lett. 38 (2009) 136.
[63] X. Zhao, Y. Shi, T. Wang, Y. Cai, G. Jiang, J. Chromatogr. A 1188 (2008) 140.
[64] S.A. Corr, Y.P. Rakovich, Y.K. Gun'ko, Nanoscale Res. Lett. 3 (2008) 87.
[65] X. You, R. He, F. Gao, J. Shao, B. Pan, D. Cui, Nanotechnol. 18 (2007) 035701.
[66] H. Lu, G. Yi, S. Zhao, D. Chen, L.-H. Guo, J. Cheng, J. Mater. Chem. 14 (2004) 1336.
[67] J. Wu, Z. Ye, G. Wang, J. Yuan, Talanta 72 (2007) 1693.
[68] W.C. Wang, Q. Zhang, B.B. Zhang, D.N. Li, X.Q. Dong, L. Zhang, J. Chang, Chin. Sci. Bull. 53 (2008) 1165.
[69] L. Li, D. Chen, Y. Zhang, Z. Deng, X. Ren, X. Meng, F. Tang, J. Ren, L. Zhang, Nanotechnology 18 (2007) 405102.
[70] C. Ren, J. Li, X. Chen, Z. Hu, D. Xue, Nanotechnology 18 (2007) 345604.
[71] Q. Chang, L. Zhu, C. Yu, H. Tang, J. Lumin. 128 (2008) 1890.
[72] P. Li, A.M. Zhu, Q.L. Liu, Q.G. Zhang, Ind. Eng. Chem. Res. 47 (2008) 7700.
[73] M.A. El-Sayed, Acc. Chem. Res. 34 (2001) 257.
[74] J. Yguerabide, E.E. Yguerabide, Anal. Biochem. 262 (1998) 137.
[75] J. Yguerabide, E.E. Yguerabide, Anal. Biochem. 262 (1998) 157.
[76] J. Turkevitch, P.C. Stevenson, J. Hillier, Faraday Soc. 11 (1951) 55.
[77] M. Brust, M. Walker, D. Bethell, D.J. Schiffrin, R. Whyman, J. Chem. Soc., Chem. Commun. (1994) 801.
[78] J.M. Kohler, J. Wagner, J. Albert, J. Mater. Chem. 15 (2005) 1924.
[79] A. Henglein, M. Giersig, J. Phys. Chem. B 103 (1999) 9533.
[80] C.S. Lin, M.R. Khan, S.D. Lin, J. Colloid Interf. Sci. 299 (2006) 678.
[81] X.S. Shen, G.Z. Wang, X. Hong, W. Zhu, Chin. J. Chem. Phys. 22 (2009) 440.
[82] S. Link, Z.L. Wang, M.A. El-Sayed, J. Phys. Chem. B 103 (1999) 3529.
[83] C.M. Goodman, V.M. Rotello, Mini-Rev. Org. Chem. 1 (2004) 103.
[84] L.M. Liz-Marzán, M. Giersig, P. Mulvaney, Langmuir 12 (1996) 4329.
[85] N.R. Jana, C. Earhart, J.Y. Ying, Chem. Mater. 19 (2007) 5074.
[86] Y.H. Lin, C.W. Liu, H.T. Chang, Anal. Methods 1 (2009) 14.
[87] P.C. Chen, S.C. Mwakwari, A.K. Oyelere, Nanotech. Sci. Appl., I (2008) 45.
[88] S. Roux, B. Garcia, J.L. Bridot, M. Salome, C. Marquette, L. Lemelle, P. Gillet, L. Blum, P. Perriat, O. Tillement, Langmuir 21 (2005) 2526.
[89] B.I. Ipe, K. Yoosaf, K.G. Thomas, J. Am. Chem. Soc. 128 (2006) 1907.
[90] K. Hu, D. Lan, X. Li, S. Zhang, Anal. Chem. 80 (2008) 9124.
[91] J. Bao, W. Chen, T. Liu, Y. Zhu, P. Jin, L. Wang, J. Liu, Y. Wei, Y. Li, ACS Nano 1 (2007) 293.
[92] C.H. Liang, C.C. Wang, Y.C. Lin, C.H. Chen, C.H. Wong, C.Y. Wu, Anal. Chem. 81 (2009) 7750.
[93] Y.C. Lin, B.Y. Yu, W.C. Lin, S.H. Lee, H. Kuo, J.J. Shyue, J. Colloid Interf. Sci. 340 (2009) 126.
[94] X. Shi, S.H. Wang, M.E. Van Antwerp, X. Chen, J.R. Baker Jr., Analyst 134 (2009) 1373.
[95] A.K. Boal, V.M. Rotello, J. Am. Chem. Soc. 122 (2000) 734.
[96] G. Schneider, G. Decher, Nano Lett. 4 (2004) 1833.
[97] A. Cruz, I. Rivero, E. Andrés, M.E. Diaz-Garcia, Anal. Bioanal. Chem. 391 (2008) 807.
[98] E.S. Shibu, M.A.H. Muhammed, K. Kimura, T. Pradeep, Nano Res. 2 (2009) 220.
[99] S. Tyagi, F.R. Kramer, Nat. Biotechnol. 14 (1996) 303.
[100] Y. Kim, D.S. Sohn, W. Tan, Int. J. Clin. Exp. Pathol. 1 (2008) 105.
[101] B. Dubertret, M. Calame, A.J. Libchaber, Nat. Biotechnol. 19 (2001) 365.
[102] W.R. Algar, M. Massey, U.J. Krull, Trends Anal. Chem. 28 (2009) 292.
[103] D.J. Maxwell, J.R. Taylor, S. Nie, J. Am. Chem. Soc. 124 (2002) 9606.
[104] M.Y. Sha, M. Yamanaka, I.D. Walton, S.M. Norton, R.L. Stoermer, C.D. Keating, M.J. Natan, S.G. Penn, NanoBiotechnology 1 (2005) 327.
[105] S. Song, Z. Liang, J. Zhang, L. Wang, G. Li, C. Fan, Angew. Chem. 48 (2009) 8670.
[106] K.B. Cederquist, R. Stoermer Golightly, C.D. Keating, Langmuir 19 (2008) 9162.
[107] W.W. Yu, E. Chang, R. Drezek, V.L. Colvin, Biochem. Biophys. Res. Commun. 348 (2006) 781.
[108] Y. Wang, N. Herron, J. Phys. Chem. 95 (1991) 525.
[109] C.B. Murray, D.J. Norris, M.G. Bawendi, J. Am. Chem. Soc. 115 (1993) 8706.
[110] O.I. Micic, A.J. Nozik, J. Lumin. 70 (1996) 95.
[111] K. Pötschke, L. Müller-Kirsch, R. Heitz, R.L. Sellin, U.W. Pohl, D. Bimberg, N.D. Zakharov, P. Werner, Physica E 21 (2004) 606.
[112] R.E. Bailey, S. Nie, J. Am. Chem. Soc. 125 (2003) 7100.
[113] C. Soman, T. Giorgio, Nanomed.: Nanotech. Biol. Med. 5 (2009) 402.
[114] W.C.W. Chan, S. Nie, Science 281 (1998) 2016.
[115] S. Mazumder, Rajib Dey, M.K. Mitra, S. Mukherjee, G.C. Das, J. Nanomater., Vol. 2009 (2009) Article ID 815734.
[116] T. Jamieson, R. Bakhshi, D. Petrova, R. Pocock, M. Imani, A.M. Seifalian, Biomaterial 28 (2007) 4717.
[117] Q. Huo, Colloid Surf. B 59 (2007) 1.
[118] D. Bodas, C. Khan-Malek, Sens. Actuator B-Chem. 128 (2007) 168.
[119] A. Scherer, H.G. Craighead, Appl. Phys. Lett. 49 (1986) 1284.
[120] J. Yang, S.R. Dave, X. Gao, J. Am. Chem. Soc. 130 (2008) 5286.
[121] L.H. Li, P. Ridha, G. Patriarche, N. Chauvin, A. Fiore, Appl. Phys. Lett. 92 (2008) 121102.
[122] A.A. Ikram, D.T. Crouse, M.M. Crouse, Mater. Lett. 61 (2007) 3666.
[123] Y.F. Shi, P. He, X.Y. Zhu, Mater. Res. Bull. 43 (2008) 2626.
[124] C.Q. Zhu, P. Wang, X. Wang, Y. Li, Nanoscale Res. Lett. 3 (2008) 213.
[125] S.O. Oluwafemi, N. Revaprasadu, A.J. Ramirez, J. Cryst. Growth 310 (2008) 3230.
[126] J.V. Williams, C.N. Adams, N.A. Kotov, P.E. Savage, Eng. Chem. Res. 46 (2007) 4358.
[127] S.Mazumder, R. Dey, M.K. Mitra, S. Mukherjee, G.C. Das, J. Nanomater. Vol. 2009 (2009) Article ID 815734.
[128] J. Lovric, H.S. Bazzi, Y. Cuie, G.R. Fortin, F.M. Winnik, D. Maysinger, J. Mol. Med. 83 (2005) 377.
[129] A.M. Derfus, W.C.W. Chan, S.N. Bhatia, Nano Lett. 4 (2004) 11.
[130] M. Green, E. Howman, Chem. Commun. (2005) 121.
[131] Y. Jin, S. Kannan, M. Wu, J.X. Zhao, Chem. Res. Toxicol. 20 (2007) 1126.
[132] C. Kirchner, T. Liedl, S. Kudera, T. Pellegrino, J.A. Munoz, H.E. Gaub, S. Stolzle, N. Fertig, W.J. Parak, Nano Lett. 5 (2005) 331.
[133] D. Gerion, F. Pinaud, S.C. Williams, W.J. Parak, D. Zanchet, S. Weiss, A.P. Alivisatos, J. Phys. Chem. B 105 (2001) 8861.
[134] M.J. Ruedas-Rama, X. Wang, E.A.H. Hall, Chem. Commun. (2007) 1544.

[135] I.L. Medintz, A.R. Clapp, F.M. Brunel, T. Tiefenbrunn, H.T. Uyeda, E.L. Chang, J.R. Deschamps, P.E. Dawson, H. Mattoussi, Nature Mater. 5 (2006) 581.
[136] R.A. Potyrailo, A.M. Leach, Appl. Phys. Lett. 88 (2006) 134110.
[137] C.I. Lin, A.K. Joseph, C.K. Changa, Y.D. Lee, Biosens. Bioelect. 20 (2004) 127.
[138] H.Y. Lin, M.S. Ho, M.H. Lee, Biosens. Bioelect. 25 (2009) 579.
[139] S.E. Diltemiz, R. Say, S. Büyüktiryaki, D. Hür, A. Denizli, A. Ersöz, Talanta 75 (2008) 890.
[140] P. Turkewitsch, B. Wandelt, G.D. Darling, W.S. Powell, Anal. Chem. 70 (1998) 2771.
[141] C.I. Lin, A.K. Joseph, C.K. Chang, Y.D. Lee, J. Chromatogr. A 1027 (2004) 259.
[142] C.I. Lin, A.K. Joseph, C.K. Chang, Y.D. Lee, Biosens. Bioelect. 20 (2004) 127.
[143] D.A. Schwartz, N.S. Norberg, Q.P. Nguyen, J.M. Parker, D.R. Gamelin, J. Am. Chem. Soc. 125 (2003) 13205.
[144] V.I. Klimov, L.P. Balet, M. Achermann, J.A. Hollingsworth, H. Kim, J. Am. Chem. Soc. 127 (2005) 544.
[145] M. Nirmal, B.O. Dabbousi, M.G. Bawendi, J.J. Macklin, J.K. Trautman, T.D. Harris, L.E. Brus, Nature 383 (1996) 802.
[146] X. Wang, X. Ren, K. Kahen, M.A. Hahn, M. Rajeswaran, S. Maccagnano-Zacher, J. Silcox, G.E. Cragg, A.L. Efros, T.D. Krauss, Nature 459 (2009) 686.
[147] B. Mahler, P. Spinicelli, S. Buil, X. Quelin, J.P. Hermier, B. Dubertret, Nat. Mater. 7 (2008) 659.
[148] W.J. Jin, M.T. Fernández-Argüelles, J.M. Costa-Fernández, R. Pereiro, A. Sanz-Medel, Chem. Commun. (2005) 883.
[149] M.A. Hahn, J.S. Tabb, T.D. Krauss, Anal. Chem. 77 (2005) 4861.
[150] Y. Chen, Z. Rosenzweig, Anal. Chem. 74 (2002) 5132.
[151] H.Y. Xie, J.G. Liang, Z.L. Zhang, Y. Liu, Z.K. He, D.W. Pang, Spectrochim. Acta Part A: Mol. Biomol. Spectr. 60 (2004) 2527.
[152] W.J. Jin, J.M. Costa-Fernández, R. Pereiro, A. Sanz-Medel, Anal. Chim. Acta 522 (2004) 1.
[153] P.T. Snee, R.C. Somers, G.P. Nair, J.P. Zimmer, M.G. Bawendi, D.G. Nocera, J. Am. Chem. Soc. 128 (2006) 13320.
[154] M. Tomasulo, I. Yildiz, S.L. Kaanumalle, F.M. Raymo, Langmuir 22 (2006) 10284.
[155] S.S. Wong, E. Joselevich, A.T. Woolley, C.L. Cheung, C.M. Lieber, Nature 394 (1998) 52.
[156] A. Hirsch, Angew. Chem. Int. Ed. 41 (2002) 1853.
[157] D. Shi, J. Lian, P. He, L.M. Wang, W.J. Van Ooij, M. Schulz, Y.J. Liu, D.B. Mast, Appl. Phys. Lett. 81 (2002) 5216.
[158] D. Shi, J. Lian, P. He, L.M. Wang, M. Schultz, D.B. Mast, Appl. Phys. Lett. 83 (2003) 5301.
[159] J. Wang, Y. Lin, TRAC. Trends Anal. Chem 27 (2008) 619.
[160] S. Daniel, T.P. Rao, K.S. Rao, S.U. Rani, G.R.K. Naidu, H.Y. Lee, T. Kawai, Sens. Actuator B 122 (2007) 672.
[161] B.C. Satishkumar, E.M. Vogl, A. Govindaraj, C.N.R. Rao, J. Phys. D 29 (1996) 3173.
[162] K. Jiang, A. Eitan, L.S. Schadler, P.M. Ajayan, R.W. Siegel, N. Grobert, M. Mayne, M. Reyes-Reyes, H. Terrones, M. Terrones, Nano Lett. 3 (2003) 275.
[163] A.V. Ellis, K. Vijayamohanan, R. Goswami, N. Chakrapani, L.S. Ramanathan, P.M. Ajayan, G. Ramanath, Nano Lett. 3 (2003) 279.
[164] L. Jiang, L. Gao, Carbon 41 (2003) 2923.
[165] A. Fasi, I. Palinko, J.W. Seo, Z. Konya, K. Hernadi, I. Kiricsi, Chem. Phys. Lett. 372 (2003) 848.
[166] D. Mattia, G. Korneva, A. Sabur, G. Friedman, Y. Gogotsi, Nanotechnology 18 (2007) 155305.
[167] T. Kyotani, L.F. Tsai, A. Tomita, Chem. Mater. 7 (1995) 1427.
[168] B. Dembinska, P.J. Kulesza, Electrochim. Acta 54 (2009) 4682.
[169] S. Giordani, J.F. Colomer, F. Cattaruzza, J. Alfonsi, M. Meneghetti, M. Prato, D. Bonifazi, Carbon 47 (2009) 578.
[170] P. Ghosh, T.G. Spiro, J. Am. Chem. Soc. 102 (1980) 5543.
[171] D.C. Bookbinder, M.S. Wrighton, J. Electrochem. Soc. 130 (1983) 1080.
[172] W.E. Ford, M. Rodgers, J. Phys. Chem. 92 (1988) 3822.
[173] E.B. Duoss, M. Twardowski, J.A. Lewis, Adv. Mater. 19 (2007) 3485.
[174] T.A. Heimer, s.T. Dárcangelis, F. Farzad, J.M. Stipkala, G.J. Meyer, Inorg. Chem. 35 (1996) 5319.
[175] P. Pechy, P.F. Rotzinger, M.K. Nazeeruddin, O. Kohle, S.M. Zakeeruddin, R. Humphry-Baker, M. Grätzel, J. Chem. Soc. Chem. Commun. (1995) 65.
[176] G. Alberti, F. Marmottini, S. Murcia-Mascaros, R. Vivani, Angew. Chem. Int. Ed. Engl. 33 (1994) 1594.
[177] M. Nagtegaal, J. Küther, J. Ensling, P. Gütilich, W. Tremel, J. Mater. Chem. 9 (1999) 1115.
[178] M.N. Tahir, M. Eberhardt, H.A. Therese, U. Kolb, P. Theato, W.E.G. Müller, H.C. Schröder, W. Tremel, Angew. Chem. Int. Ed. 45 (2006) 4803.
[179] M.N. Tahir, M. Eberhardt, P. Theato, S. Faiss, A. Janshoff, T. Gorelik, U. Kolb, W. Tremel, Angew. Chem. Int. Ed. 45 (2006) 908.
[180] M.N. Tahir, N. Zink, M. Eberhardt, H.A. Therese, S. Faiss, A. Janshoff, U. Kolb, P. Theato, W. Tremel, Small 3 (2007) 829.
[181] F. Zhang, D. Zhao, Nano Res. 2 (2009) 292.
[182] Y. Jin, A. Li, S.G. Hazelton, S. Liang, C.L. John, P.D. Selid, D.T. Pierce, J.X. Zhao, Coord. Chem. Rev. 253 (2009) 2998.
[183] L. Wang, W. Zhao, W. Tan, Nano Res. 1 (2008) 99.
[184] L.H. Allen, E. Matijevic, J. Colloid Interf. Sci. 31 (1969) 287.
[185] J. Depasse, A. Watillon, J. Colloid Interf. Sci. 33 (1970) 430.
[186] R.K. Iler, The Chemistry of Silica, Wiley, New York, 1979.
[187] W. Stöber, A. Fink, E. Bohn, J. Colloid Interf. Sci 26 (1968) 6212.
[188] F.J. Arriagada, K. Osseo-Asare, J. Colloid Interf. Sci. 170 (1995) 8.
[189] T.R. Sathe, A. Agrawal, S. Nie, Anal. Chem. 78 (2006) 5627.
[190] D. Gao, Z. Wang, B. Liu, L. Ni, M. Wu, Z. Zhang, Anal. Chem. 80 (2008) 8545.
[191] M. Arduini, F. Mancin, P. Tecilla, U. Tonellato, Langmuir 23 (2007) 8632.
[192] S.H. Kim, J. Jeyakumar, J.A. Katzenellenbogen, J. Am. Chem. Soc. 129 (2007) 13254.
[193] A.L. Lisenbigler, G. Lu, J.T. Yates, Chem. Rev. 95 (1995) 735–758.
[194] D. Chatterjee, S. Dasgupta, J. Photochem. Photobiol. C 6 (2005) 186.
[195] K.T. Lim, H.S. Hwang, W. Ryoo, K.P. Johnston, Langmuir 20 (2004) 2466.
[196] J. Eastoe, M.J. Hollamby, L. Hudson, Adv. Colloid Interf. Sci. 128–130 (2006) 5.
[197] R. Inaba, T. Fukahori, M. Hamamoto, T. Ohno, J. Mol. Catal. A: Chem. 260 (2006) 247.
[198] M. Luo, K. Cheng, W. Weng, C. Song, P. Du, G. Shen, G. Xu, G. Han, Mater. Lett. 62 (2008) 1965.
[199] R.J. Tayade, R.G. Kulkarni, R.V. Jasra, Ind. Eng. Chem. Res. 45 (2006) 922.
[200] S. Eiden-Assmann, J. Widoniak, G. Maret, Chem. Mater. 16 (2004) 6.
[201] T. Sugimoto, X. Zhou, A. Muramatsu, J. Coll. Interf. Sci. 259 (2003) 53.
[202] G. Oskam, A. Nellore, R.L. Penn, P.C. Searson, J. Phys. Chem. B 107 (2003) 1734.
[203] H. Yang, K. Zhang, R. Shi, X. Li, X. Dong, Y. Yu, J. Alloy Compd. 413 (2006) 302.
[204] H. Zhang, J.F. Banfield, Chem. Mater. 17 (2005) 3421.
[205] K. Mori, K. Maki, S. Kawasaki, S. Yuan, Hi. Yamashita, Chem. Eng. Sci. 63 (2008) 5066.
[206] J. Zhang, X. Xiao, J. Nan, J. Hazard. Mater. 176 (2010) 617.
[207] H.H. Ou, S.L. Lo, Sep. Puri. Technol. 58 (2007) 179.
[208] T. Kasuga, M. Hiramatsu, A. Hoson, T. Sekino, K. Niihara, Adv. Mater. 11 (1999) 1307.
[209] G.H. Du, Q. Chen, R.C. Che, Z.Y. Yuan, L.M. Peng, Appl. Phys. Lett. 79 (2001) 3702.
[210] C.S. Kim, B.K. Moon, J.H. Park, B.C. Choi, H.J. Seo, J. Cryst. Growth 257 (2003) 309.
[211] C.S. Kim, B.K. Moon, J.H. Park, S.T. Chung, S.M. Son, J. Cryst. Growth 254 (2003) 405.
[212] R.K. Wahi, Y. Liu, J.C. Falkner, V.L. Colvin, J. Colloid Interf. Sci. 302 (2006) 530.
[213] B. Wen, C. Liu, Y. Liu, Inorg. Chem. 44 (2005) 6503.
[214] Y.T. Shi, R. Yuan, Y.Q. Chai, X.L. He, Electrochim. Acta 52 (2007) 3518.
[215] E. Llobet, E.H. Espinosa, E. Sotter, R. Ionescu, X. Vilanova, J. Torres, A. Felten, J.J. Pireaux, X. Ke, G. Van Tendeloo, F. Renaux, Y. Paint, M. Hecq, C. Bittencourt, Nanotechnology 19 (2008) 375501.
[216] X. Pang, D. He, S. Luo, Q. Cai, Sens. Actuators B 137 (2009) 134.
[217] R. Bazzi, M.A. Flores, C. Louis, K. Lebbou, W. Zhang, C. Dujardin, S. Roux, B. Mercier, G. Ledoux, E. Bernstein, P. Perriat, O. Tillement, J. Colloid Interf. Sci. 273 (2004) 191.
[218] C. Louis, K. Lebbou, M.A. Flores-Gonzalez, R. Bazzi, B. Hautefeuille, B. Mercier, S. Roux, P. Perriat, C. Olagnon, O. Tillement, J. Cryst. Growth 265 (2004) 459.
[219] M. Flores-Gonzalez, G. Ledoux, S. Roux, K. Lebbou, P. Perriat, O. Tillement, J. Solid State Chem. 178 (2005) 989.
[220] M.A. Flores-Gonzalez, C. Louis, R. Bazzi, G. Ledoux, K. Lebbou, S. Roux, P. Perriat, O. Tillement, Appl. Phys. A-Mater. Sci. Process. A81 (2005) 1385.
[221] C. Louis, S. Roux, G. Ledoux, C. Dujardin, O. Tillement, B. Cheng, P. Perriat, Chem. Phys. Lett. 429 (2006) 157.
[222] M. Nichkova, D. Dosev, S.J. Gee, B.D. Hammock, I.M. Kennedy, Anal. Bioanal. Chem. 384 (2006) 631.
[223] M. Nichkova, D. Dosev, S.J. Gee, B.D. Hammock, I.M. Kennedy, Anal. Chem. 77 (2005) 6864.
[224] C. Louis, R. Bazzi, C.A. Marquette, J.L. Bridot, S. Roux, G. Ledoux, B. Mercier, L. Blum, P. Perriat, O. Tillement, Chem. Mater. 17 (2005) 1673.
[225] K. Binnemans, Chem. Rev. 109 (2009) 4283.
[226] P.A. McCarron, A.M. Faheem, Nanomedicine 5 (2010) 3.
[227] M.E. Gindy, R.K. Prud'homme, Expert Opin. Drug Deliv. 6 (2009) 865.
[228] J. Gao, H. Gu, B. Xu, Acc. Chem. Res. 42 (2009) 1097.
[229] S. Roux, O. Tillement, C. Billotey, J.L. Coll, G. Le Duc, C.A. Marquette, P. Perriat, Intern. J. Nanotechnol. 7 (2010) 781.
[230] M. Liong, S. Angelos, E. Choi, K. Patel, J.F. Stoddart, J.I. Zink, J. Mater. Chem. 19 (2009) 6251.
[231] M.R. Gwinn, V. Vallyathan, Environ. Health Perspect. 114 (2006) 1818.
[232] M.A. Albrecht, C.W. Evans, C.L. Raston, Green Chem. 8 (2006) 417.
[233] R. Brayner, Nanotoday 3 (2008) 48.